# Boryl-Metal Bonds Facilitate Cobalt/Nickel-Catalyzed Olefin Hydrogenation

Tzu-Pin Lin and Jonas C. Peters*

Division of Chemistry and Chemical Engineering, California Institute of Technology, Pasadena, California 91125, United States

SUPPORTING INFORMATION

**This PDF file includes:**

**Experimental procedures**

**Figure S1.** $^{1}$H NMR spectrum of **[($^{Cy}$PBP)CoH]$_2$** (**1**) in $C_6D_6$ under 1 atm $N_2$ at 298 K.

**Figure S2.** Top: $^{1}$H NMR spectrum of **[($^{Cy}$PBHP)CoH]$_2$** (**1**-$H_2$) in $C_6D_6$ under 1 atm $H_2$ at 298 K. Bottom: $^{1}$H NMR spectrum of **[($^{Cy}$PBDP)CoD]$_2$** (**1**-$D_2$) in $C_6D_6$ under 1 atm $D_2$ at 298 K.

**Figure S3.** $^{1}$H NMR spectrum of **[($^{Cy}$PBP)CoH]$_2$[PF$_6$]** ([**2**][$PF_6$]) in $C_6D_6$ under 1 atm $N_2$ at 298 K.

**Figure S4.** $^{1}$H, $^{31}$P, $^{11}$B, and $^{13}$C NMR spectra of **[($^{Ph}$PBP)Ni]$_2$** (**3**) in THF-$d_8$ under 1 atm $N_2$ at 298 K.

**Figure S5.** $^{1}$H, $^{31}$P, $^{11}$B, and $^{13}$C NMR spectra of **[($^{Ph}$PBHP)NiH]$_2$** (**4**) in THF-$d_8$ under 1 atm $H_2$ at 298 K.

**Figure S6.** Top: $^{1}$H (green) and $^{1}$H{$^{31}$P} (maroon) NMR spectra of **[($^{Ph}$PBHP)NiH]$_2$** (**4**) in THF-$d_8$ under 1 atm $H_2$ at 298 K. Bottom: $^{1}$H (green) and $^{1}$H{$^{11}$B} (maroon) NMR spectra of **[($^{Ph}$PBHP)NiH]$_2$** (**4**) in THF-$d_8$ under 1 atm $H_2$ at 298 K.

**Figure S7.** Determination of $T_1$(min) for the B-H and Ni-H resonances in **[($^{Ph}$PBHP)NiH]$_2$** (**4**).

**Figure S8.** $^{1}$H, $^{31}$P, $^{11}$B, and $^{13}$C NMR spectra of **($^{tBu}$PBP)NiCl** (**5**) in $C_6D_6$ under 1 atm $N_2$ at 298 K.

**Figure S9.** $^{1}$H, $^{31}$P, $^{11}$B, $^{19}$F, and $^{13}$C NMR spectra of **($^{tBu}$PBP)NiOTf** (**6**) in $C_6D_6$ under 1 atm $N_2$ at 298 K.

**Figure S10.** $^{1}$H, $^{31}$P, $^{11}$B, and $^{13}$C NMR spectra of **($^{tBu}$PBP)NiH** (**7**) in $C_6D_6$ under 1 atm $N_2$ at 298 K.

**Figure S11.** $^{1}$H, $^{31}$P, $^{11}$B, and $^{13}$C NMR spectra of **($^{tBu}$PBP)NiOC(H)O** (**8**) in $C_6D_6$ under 1 atm $N_2$ at 298 K.

**Figure S12.** $^{1}$H DOSY NMR spectra of **[($^{Cy}$PBP)CoH]$_2$** (**1**, top), **[($^{Cy}$PBHP)CoH]$_2$** (**1**-$H_2$, middle), and **($^{tBu}$PBP)NiCl** (**5**, bottom) in $C_6D_6$ at 298 K. (The calculated diffusion coefficients are based on the following report: Evans, R.; Deng, Z.; Rogerson, A. K.; McLachlan, A. S.; Richards, J. J.; Nilsson, M.; Morris, G. A. *Angew. Chem. Int. Ed.* 2013, *52*, 3199-3202.)

**Figure S13.** Top: Thin film ATR-IR spectra of ligand **$^{Cy}$PB(H)P** and **[($^{Cy}$PBP)CoH]$_2$** (**1**). Bottom: Solution IR (KBr) spectrum of **[($^{Cy}$PBP)CoH]$_2$** (**1**) in $C_6H_6$.

**Figure S14.** Thin film ATR-IR spectrum (blue) of **[($^{Cy}$PBHP)CoH]$_2$** (**1**-$H_2$) under 1 atm $H_2$. The conversion of **[($^{Cy}$PBHP)CoH]$_2$** (**1**-$H_2$) to **[($^{Cy}$PBP)CoH]$_2$** (**1**) was observed by repeatedly dissolving/reforming the thin film using $C_6H_6$ under 1 atm $N_2$.

**Figure S15.** Thin film ATR-IR spectra of **[($^{Cy}$PBP)CoH]$_2$** (**1**, black) and **[($^{Cy}$PBP)CoD]$_2$** (**1**-$d_2$, red).

**Figure S16.** Thin film ATR-IR spectra of **[($^{Cy}$PBP)CoH]$_2$** (**1**, dash trace) and **[($^{Cy}$PBP)CoH]$_2$[PF$_6$]** ([**2**][$PF_6$], solid trace).

**Figure S17.** Thin film ATR-IR spectra of ligand **$^{Ph}$PB(H)P** (dash trace) and **[($^{Ph}$PBP)Ni]$_2$** (**3**, solid trace).

**Figure S18.** Thin film ATR-IR spectra of **($^{tBu}$PBP)NiH** (**7**, dash trace) and **($^{tBu}$PBP)NiD** (**7-D**, solid trace).

**Figure S19.** Thin film ATR-IR spectra of **($^{tBu}$PBP)NiH** (**7**, dash trace) and **($^{tBu}$PBP)NiOC(H)O** (**8**, solid trace).

**Figure S20.** Left: UV-vis spectra of **[($^{Cy}$PBP)CoH]$_2$** (**1**, blue, $3.77 \times 10^{-5}$ M, 1 atm $N_2$) and **[($^{Cy}$PBHP)CoH]$_2$** (**1**-$H_2$, red, $3.77 \times 10^{-5}$ M, 1 atm $H_2$) in toluene at 293 K. Right: UV-vis spectra of **[($^{Ph}$PBP)Ni]$_2$** (**3**, blue, $3.06 \times 10^{-5}$ M, 1 atm $N_2$) and **[($^{Ph}$PBHP)NiH]$_2$** (**4**, red, $3.06 \times 10^{-5}$ M, 1 atm $H_2$) in toluene at 293 K.

**Figure S21.** The cyclic voltammogram trace acquired for **[($^{Cy}$PBP)CoH]$_2$** (**1**).

**Figure S22.** Reaction order determination by the method of initial rates for the hydrogenation of *cis*-cyclooctene catalyzed by **[($^{Cy}$PBP)CoH]$_2$** (**1**). (a) Plot of ln(rate) against ln[olefin] ([olefin]: 11.4 – 43.7 mM). (b) Plot of ln(rate) against ln[$Co_2$] ([$Co_2$]: 0.84 – 8.43 mM). (c) Plot of ln(rate) against ln[$H_2$] (pressure of $H_2$: 0.5 – 3.9 atm).

**Figure S23.** Plots of initial rates against the concentrations of olefin, catalyst **($^{tBu}$PBP)NiH** (**7**), and $H_2$ for the hydrogenation of *cis*-cyclooctene catalyzed by complex **7**. (a) Initial rates vs [olefin] (4.36 – 43.6 mM). (b) Initial rates vs [**7**] (1.14 – 11.4 mM). (c) Initial rates vs [$H_2$] (pressure of $H_2$: 0.3 – 3.9 atm).

**Figure S28.** The two singly occupied molecular orbitals (isovalue = 0.05) of complex **[($^{Cy}$PBP)CoH]$_2$** (**1**). Hydrogenation atoms are omitted for clarity.

**Figure S29.** Five natural orbitals (NOs, isovalue = 0.05) illustrating the electronic structure and the predicted $S = 1$ spin state of model complex **[($^{Me}$PBP)CoH]$_2$** ([**1'**]). The rest of the NOs (not shown) have occupancy of > 1.99 or < 0.01. Three NOs that are associated with the Co-H-Co core are NO 1-3. These orbitals are in-phase (NO 1, occupancy: 1.99), non-bonding (NO 2, occupancy: 1.00), and out-of-phase (NO 3, occupancy: 0.01) combinations of two d(Co) and one s(H) orbitals. In addition, we found a π(Co-Co) (NO 4, occupancy: 1.99) and a π*(Co-Co) (NO 5, occupancy: 1.00) orbitals. Taken collectively, the orbital occupancies of NO 2, NO 4, and NO 5 indicate the absence of a net Co-Co bond. In turn, the two Co atoms are involved in a 3c-2e interaction (NO 1) through the bridging hydride. The NO analysis also reveals that the two unpaired electrons are aligned ferromagnetically in two orthogonal π*(Co-Co) orbitals (NO 2, NO 5), leading to an $S = 1$ configuration which is in agreement with the spin-density plot shown in Figure 1.

**Figure S30.** Top: Three natural orbitals (NOs, isovalue = 0.05) illustrating the electronic structure and the predicted $S = ½$ spin state of model complex **[($^{Me}$PBP)CoH]$_2^+$** ([**2'**]$^+$). The rest of the NOs (not shown) have occupancy of > 1.99 or < 0.01. Examinations of NO 1 and NO 3 reveal that they are, respectively, symmetry related Co-Co bonding and antibonding orbitals. These results are in line with two Co being antiferromagnetically coupled (a strongly antiferromagnetically coupled system would have occupancies of 1.00/1.00 whereas a fully electronically paired system would have occupancies of 2/0). Taking linear combinations of NO 1 and NO 3 recovers two localized Co d-orbitals (Bottom). These orbitals are magnetic natural orbitals (MNOs) which could be employed to visualize magnetic interactions (also see ref 22). According to these calculations, the two Co in complex [**2**]$^+$ could be described as antiferromagnetically coupled. The unpaired electron is localized in NO 2

which has a large contribution from Co2, consistent with the experimentally obtained EPR spectrum showing hyperfine coupling to only one Co atom.

**Figure S31.** Top: Molecular orbitals (isovalue = 0.05) of complex **[($^{Me}$PBP)Ni]$_2$** (**3'**) showing the Ni-($\mu_2$-B)$_2$-Ni 4c-4e interaction (MO 155, MO 156) as well as the σ(Ni-Ni) orbital (MO 160). Hydrogen atoms are omitted for clarity. Bottom: Calculated electron density plot for **3'** with bond paths (pink), (3,-1) bond critical points (BCPs, red), and electron density (e bohr$^{-3}$, blue).

**Figure S32.** Top: Molecular orbitals (isovalue = 0.05) of complex **[($^{Me}$PBHP)NiH]$_2$** (**4'**) showing the agostic σ-borane coordination mode (MO 134, MO 137). Hydrogen atoms are omitted for clarity. Bottom: Calculated electron density plot for **4'** with bond paths (pink), (3,-1) bond critical points (BCPs, red), and electron density (e bohr$^{-3}$, blue). The absence of a bond path/BCP between B1-Ni1 and B2-Ni2 suggests that the coordination mode of the borane ligand is closer to *pseudo* agostic.

**Figure S33.** Geometry of (PH$_3$)$_2$Ni-($\mu_2$-H)$_2$-Ni(PH$_3$)$_2$ optimized at BP86/6-31g(d) level of theory by DFT. The MOs (isovalue = 0.05) illustrate the three-center-two-electron bonds as well as the presence of a π*(Ni-Ni) bond. Hydrogen atoms are omitted for clarity.

**Table S1.** Calculated EPR parameters for complex **[($^{Me}$PBP)CoH]$_2^+$** ([**2'**]$^+$) at BP86/6-31+g(d,p) level of theory.

**DFT structural coordinates**

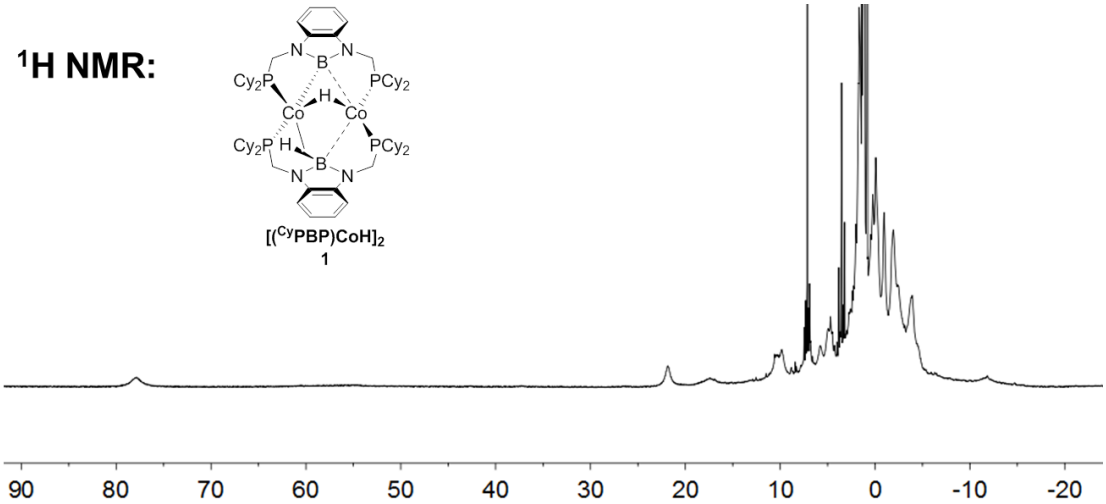


**Figure S1.** $^{1}$H NMR spectrum of **[(**$^{Cy}$**PBP)CoH]$_2$** (**1**) in $C_6D_6$ under 1 atm $N_2$ at 298 K.

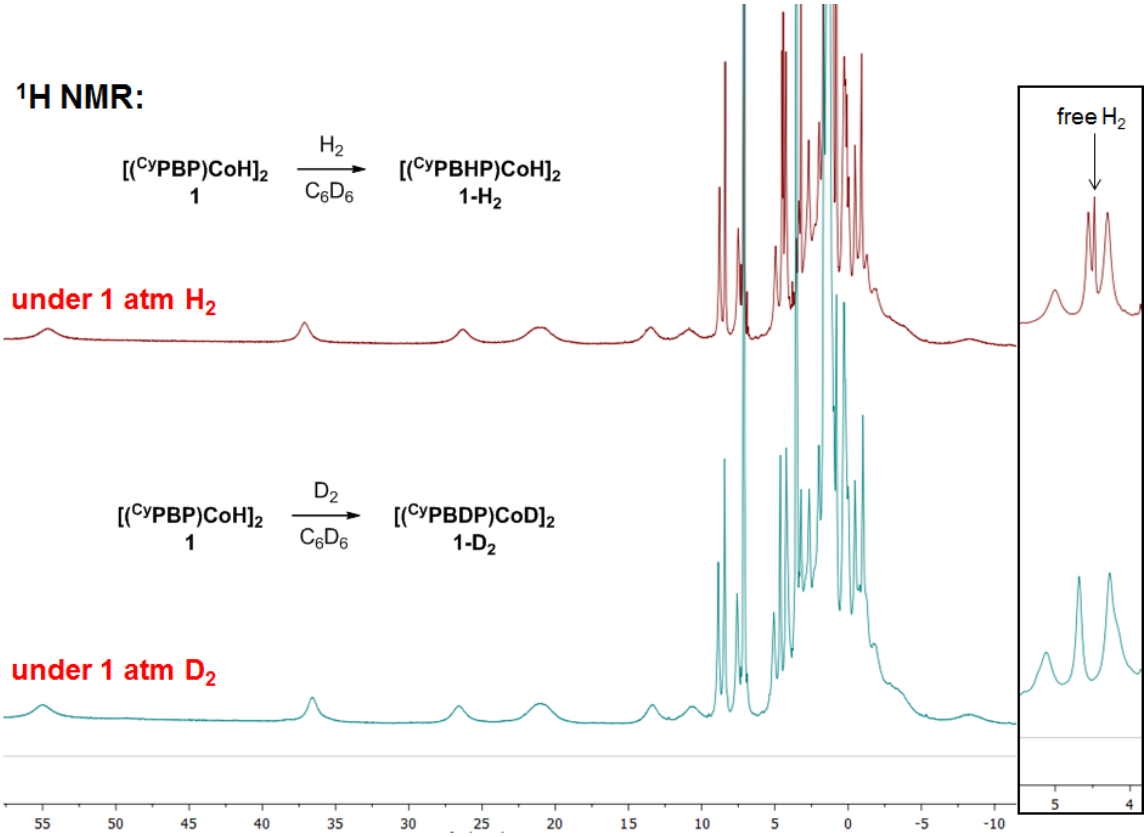


Several plausible identities for **1**-$H_2$:

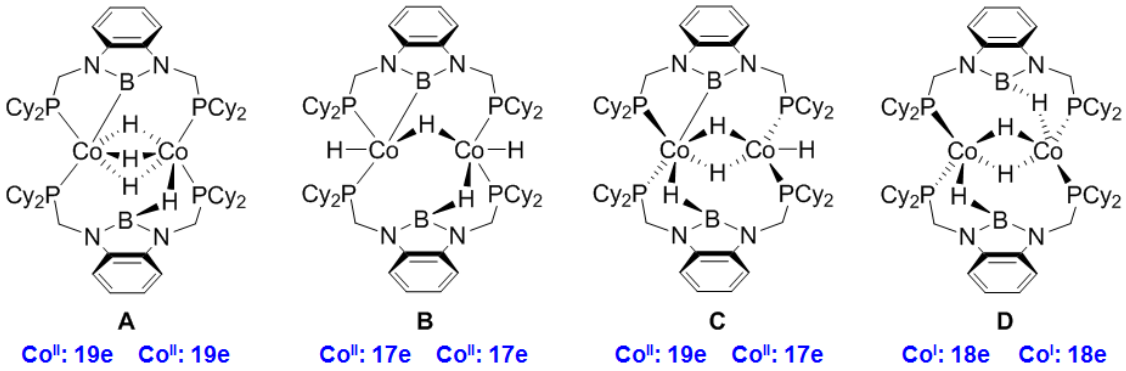


**Figure S2.** Top: $^1$H NMR spectrum of **[(**$^{Cy}$**PBHP)CoH]$_2$** (**1**-$H_2$) in $C_6D_6$ under 1 atm $H_2$ at 298 K. Bottom: $^1$H NMR spectrum of **[(**$^{Cy}$**PBDP)CoD]$_2$** (**1**-$D_2$) in $C_6D_6$ under 1 atm $D_2$ at 298 K.

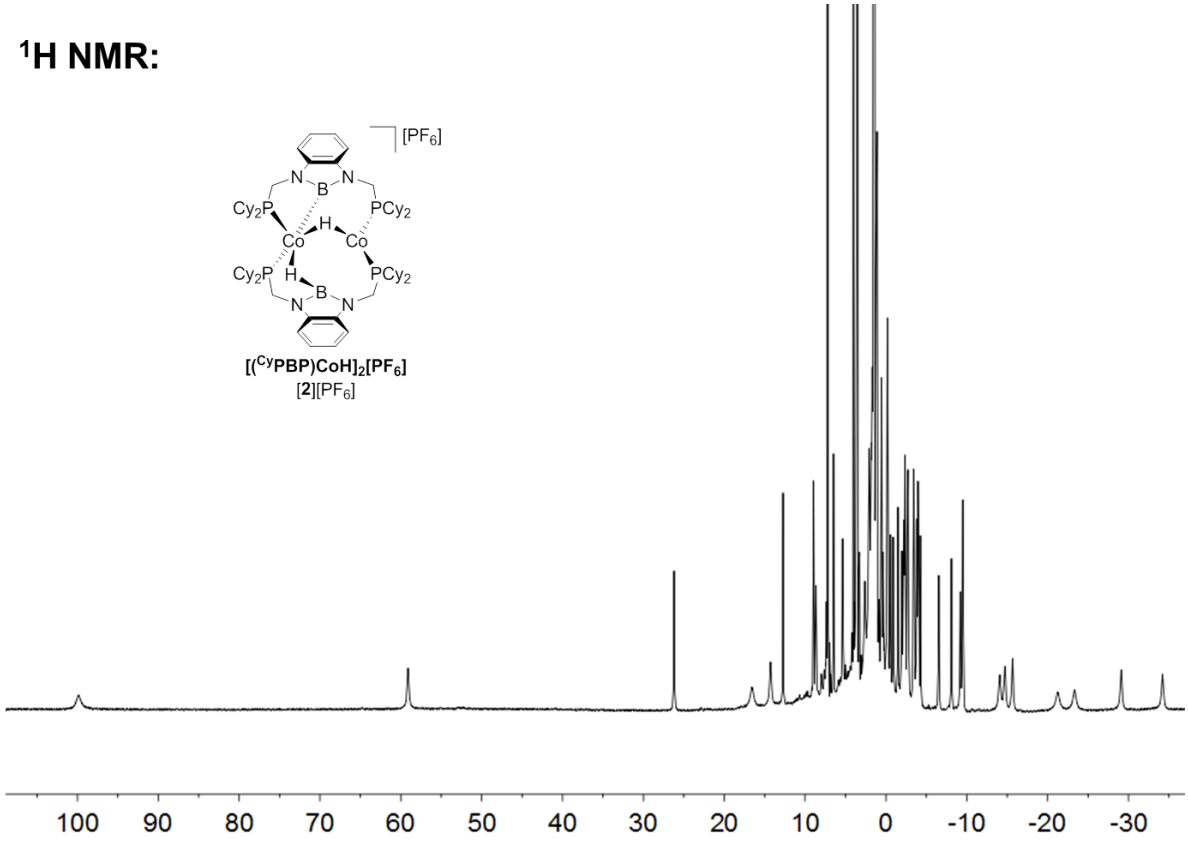


**Figure S3.** $^{1}$H NMR spectrum of **[(**$^{Cy}$**PBP)CoH]$_2$[PF$_6$]** ([**2**][PF$_6$]) in $C_6D_6$ under 1 atm $N_2$ at 298 K.

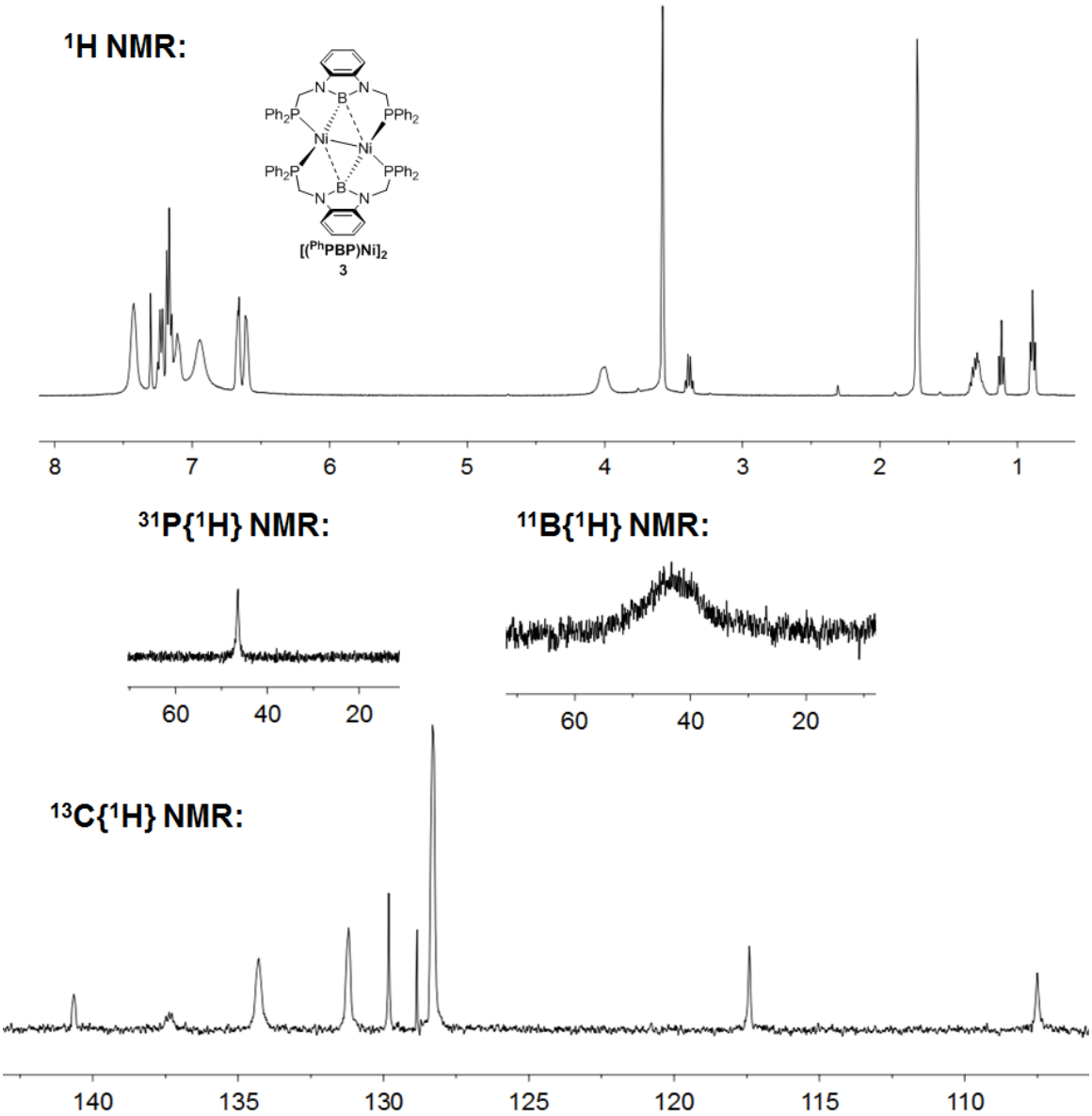


**Figure S4.** $^{1}$H, $^{31}$P, $^{11}$B, and $^{13}$C NMR spectra of **[(**$^{Ph}$**PBP)Ni]$_2$** (**3**) in THF-$d_8$ under 1 atm $N_2$ at 298 K.

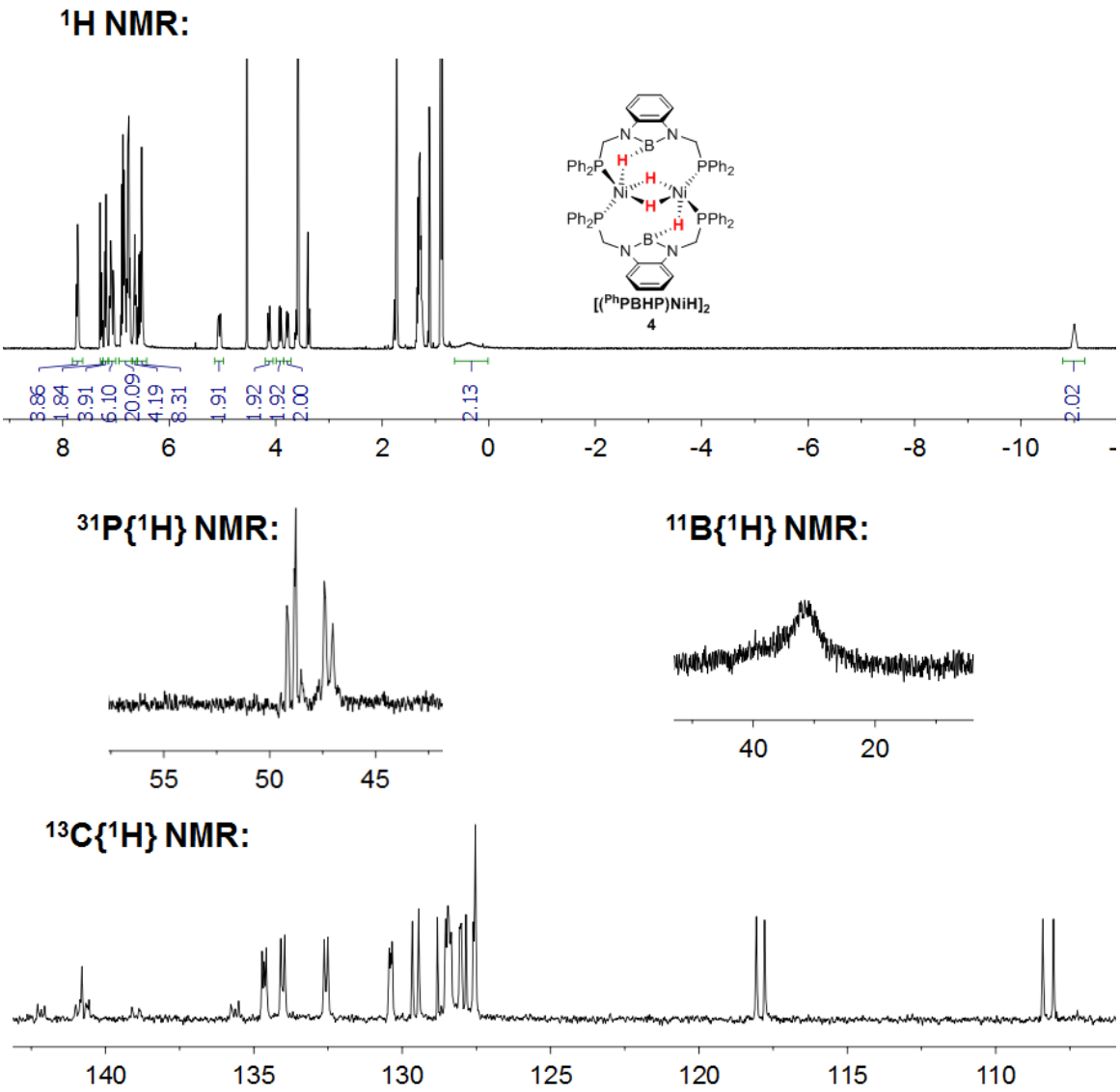


**Figure S5.** $^{1}$H, $^{31}$P, $^{11}$B, and $^{13}$C NMR spectra of **[(**$^{Ph}$**PBHP)NiH]$_2$** (**4**) in THF-$d_8$ under 1 atm $H_2$ at 298 K.

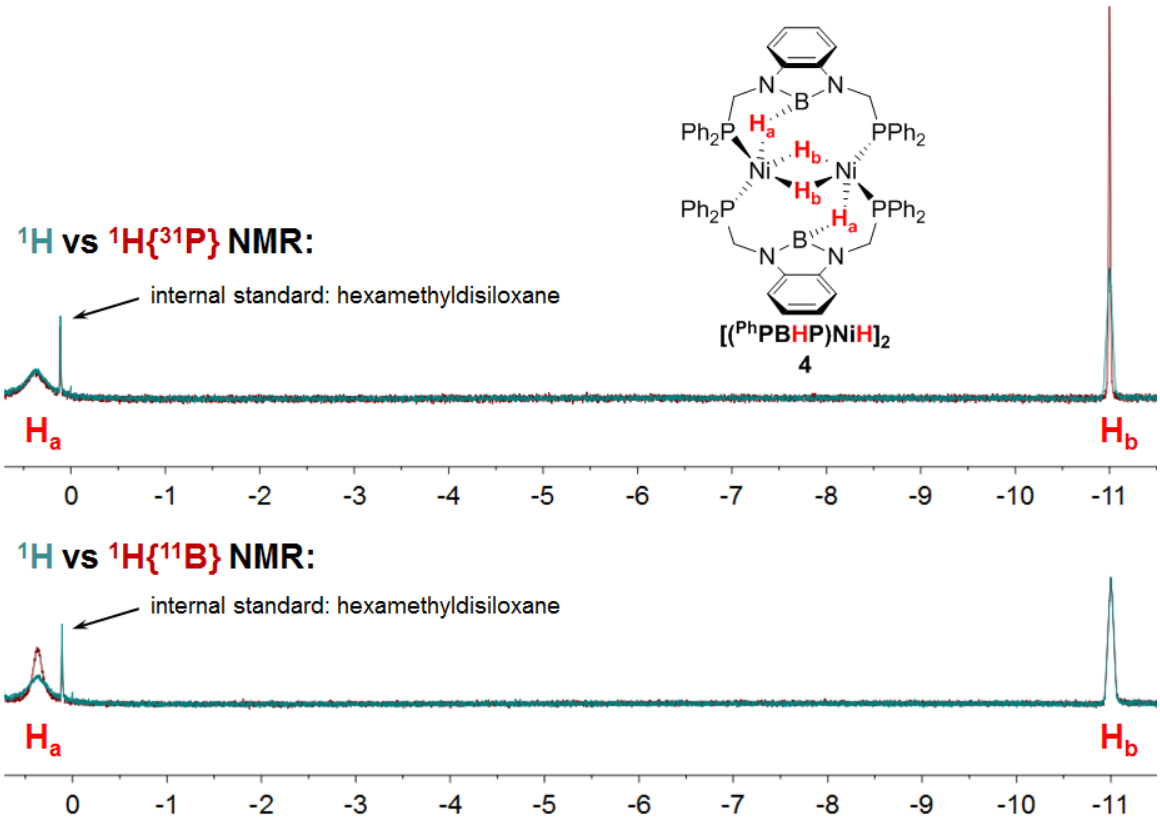


**Figure S6.** Top: $^1$H (green) and $^1$H{$^{31}$P} (maroon) NMR spectra of **[($^{Ph}$PBHP)NiH]$_2$** (**4**) in THF-$d_8$ under 1 atm $H_2$ at 298 K. Bottom: $^1$H (green) and $^1$H{$^{11}$B} (maroon) NMR spectra of **[($^{Ph}$PBHP)NiH]$_2$** (**4**) in THF-$d_8$ under 1 atm $H_2$ at 298 K.

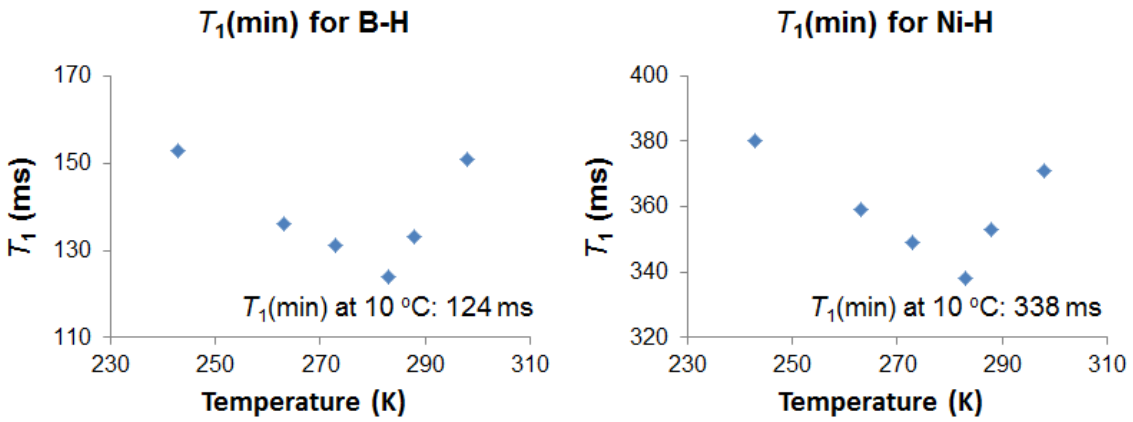


**Figure S7.** Determination of $T_1$(min) for the B-H and Ni-H resonances in **[($^{Ph}$PBHP)NiH]$_2$** (**4**).

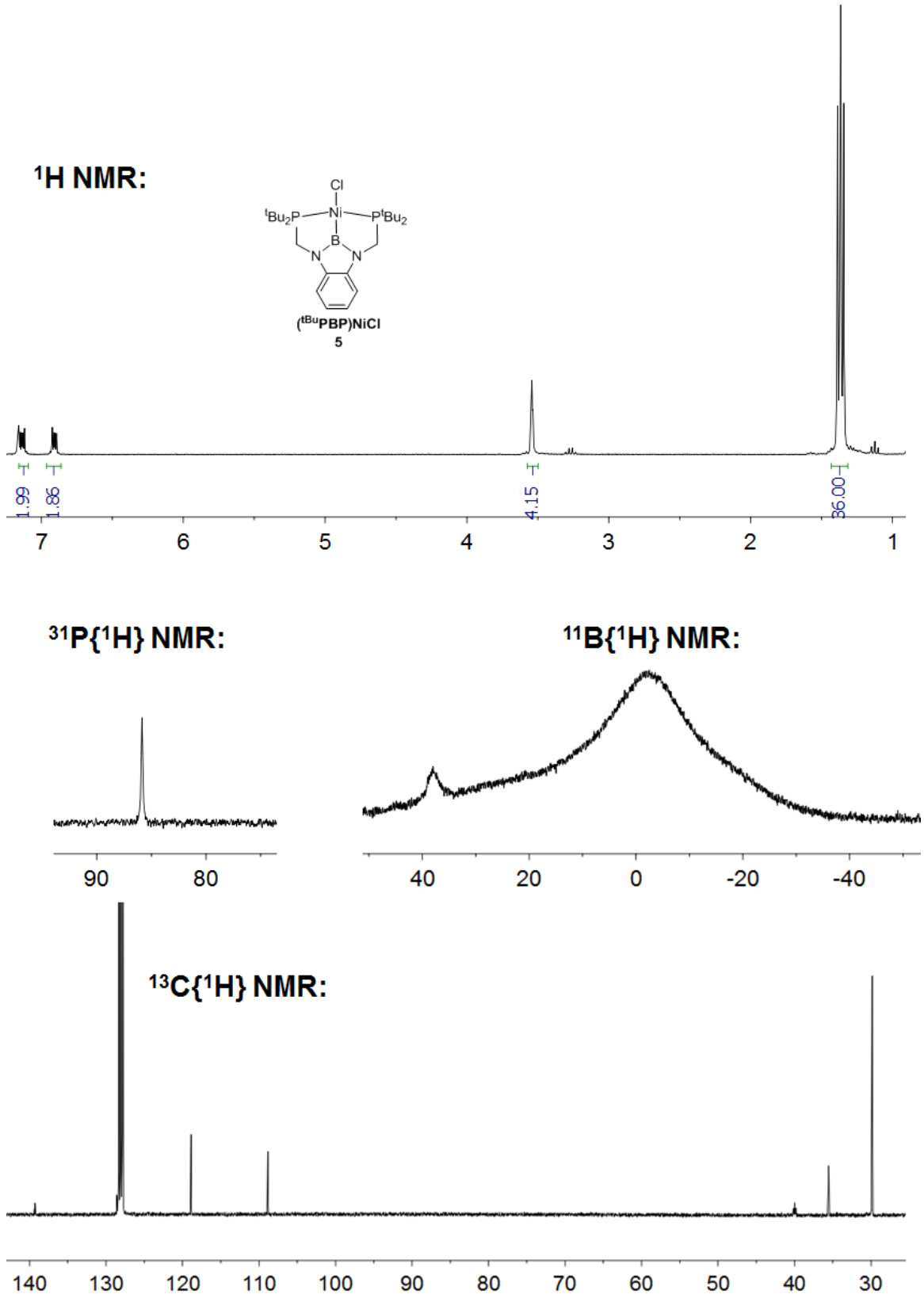


**Figure S8.** $^{1}$H, $^{31}$P, $^{11}$B, and $^{13}$C NMR spectra of **($^{tBu}$PBP)NiCl** (**5**) in $C_6D_6$ under 1 atm $N_2$ at 298 K.

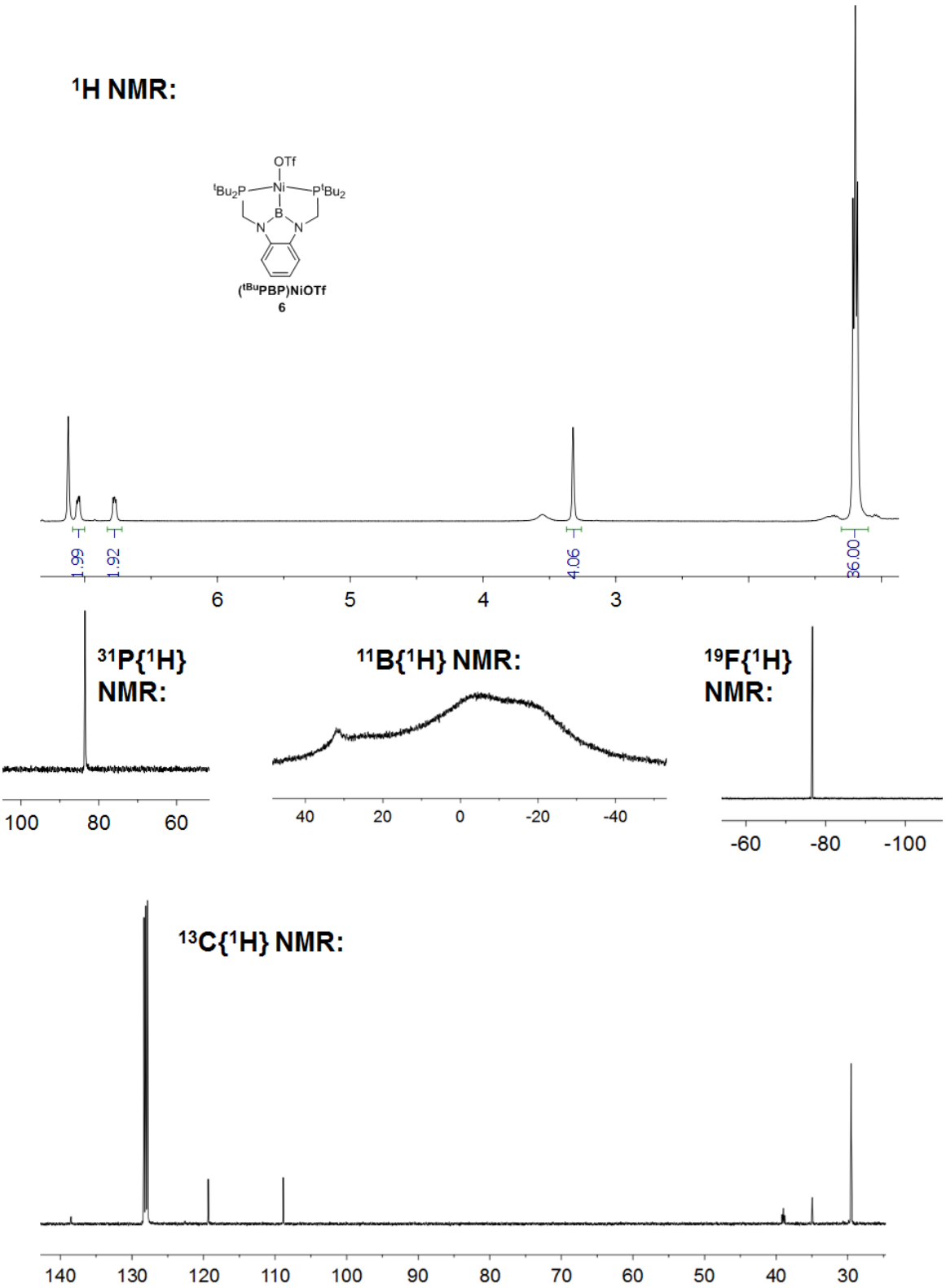


**Figure S9.** $^{1}H$, $^{31}P$, $^{11}B$, $^{19}F$, and $^{13}C$ NMR spectra of **($^{tBu}$PBP)NiOTf** (**6**) in $C_6D_6$ under 1 atm $N_2$ at 298 K.

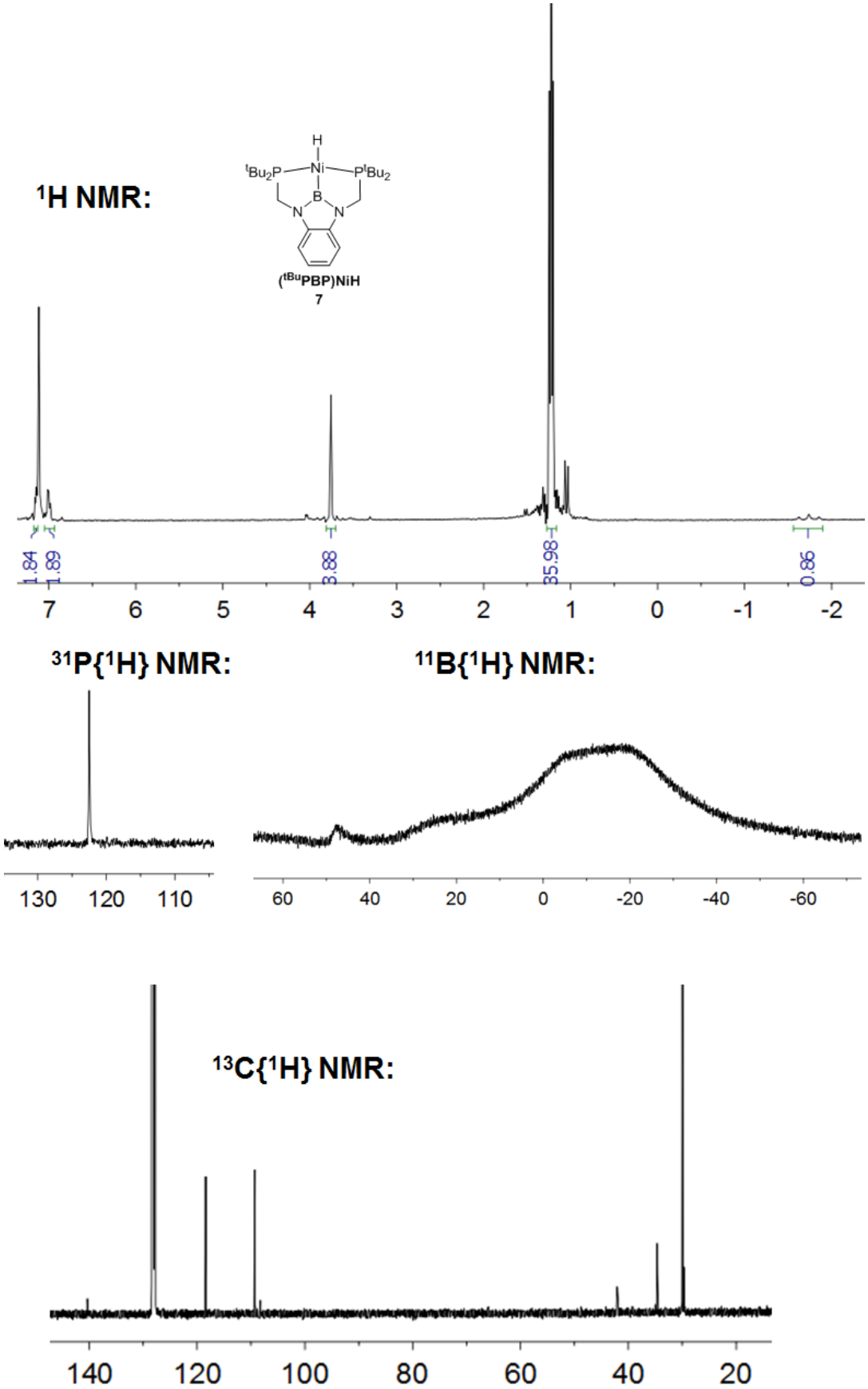


**Figure S10.** $^{1}$H, $^{31}$P, $^{11}$B, and $^{13}$C NMR spectra of **($^{tBu}$PBP)NiH** (**7**) in $C_6D_6$ under 1 atm $N_2$ at 298 K.

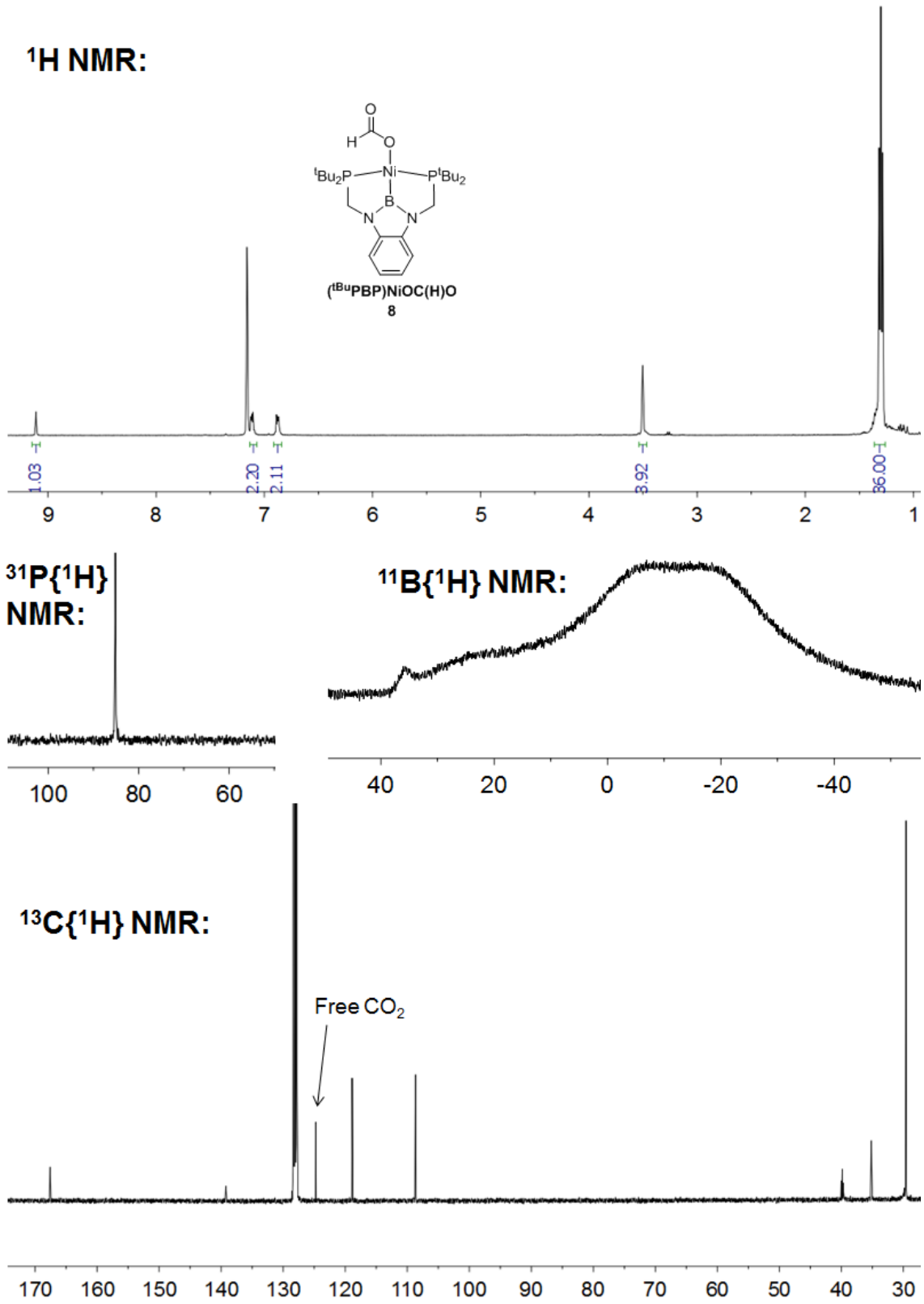


**Figure S11.** $^{1}$H, $^{31}$P, $^{11}$B, and $^{13}$C NMR spectra of **($^{t\mathrm{Bu}}$PBP)NiOC(H)O** (**8**) in $C_6D_6$ under 1 atm $N_2$ at 298 K.

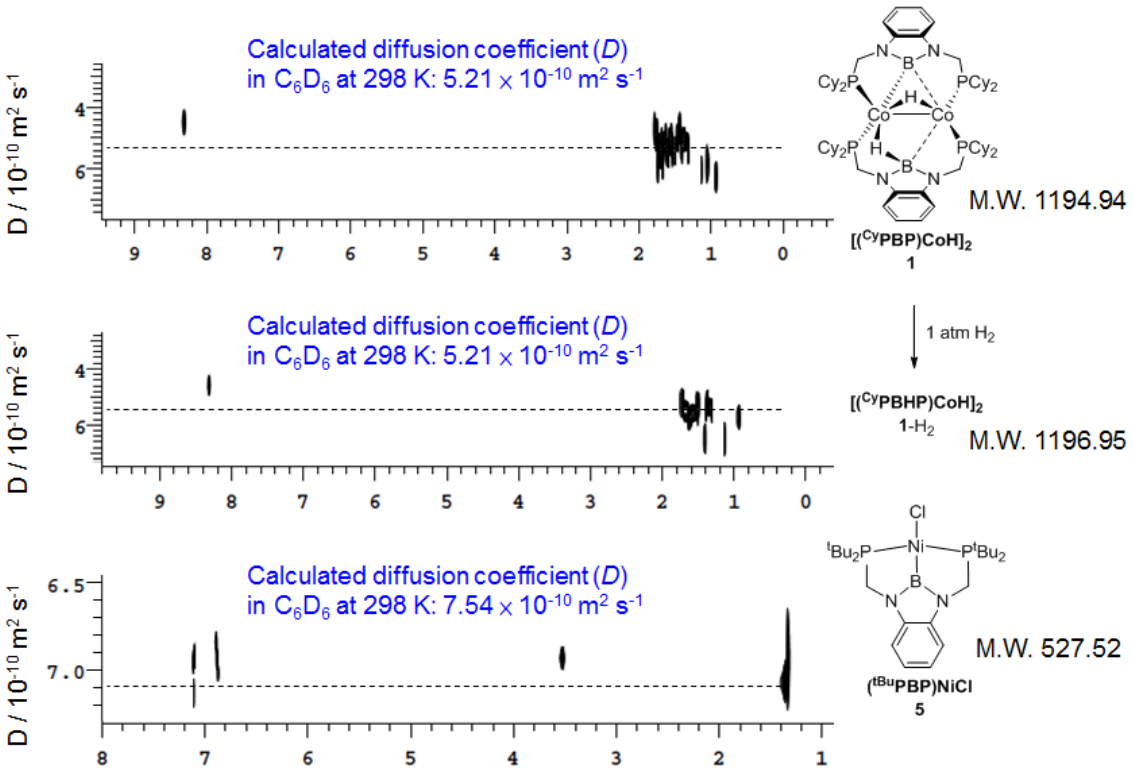


**Figure S12.** $^1$H DOSY NMR spectra of **[(**$^{Cy}$**PBP)CoH]**$_2$ (**1**, top), **[(**$^{Cy}$**PBHP)CoH]**$_2$ (**1**-$H_2$, middle), and **(**$^{tBu}$**PBP)NiCl** (**5**, bottom) in $C_6D_6$ at 298 K. (The calculated diffusion coefficients are based on the following report: Evans, R.; Deng, Z.; Rogerson, A. K.; McLachlan, A. S.; Richards, J. J.; Nilsson, M.; Morris, G. A. *Angew. Chem. Int. Ed.* 2013, *52*, 3199-3202.)

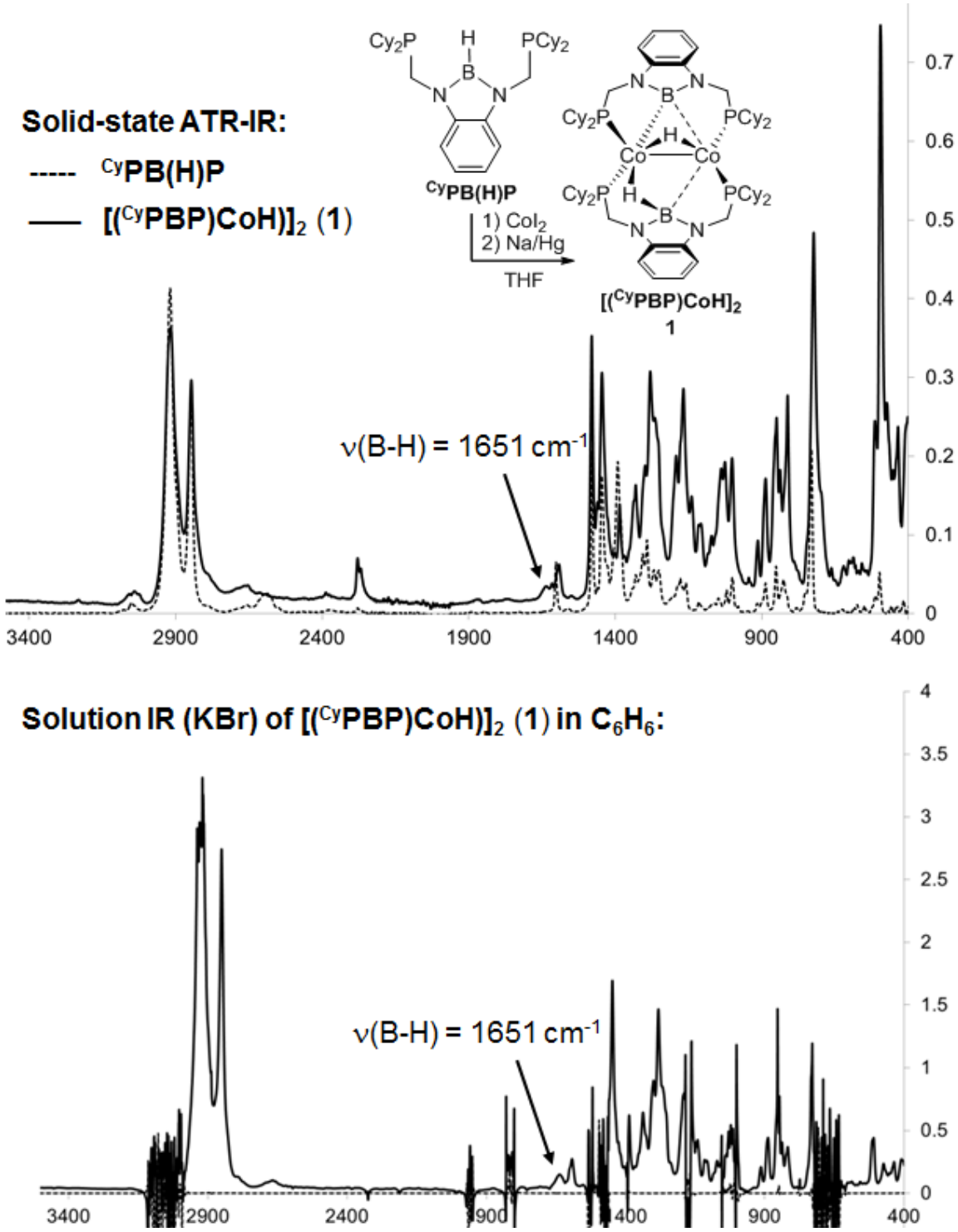


**Figure S13.** Top: Thin film ATR-IR spectra of ligand $^{Cy}$**PB(H)P** and **[(**$^{Cy}$**PBP)CoH]**$_2$ (**1**). Bottom: Solution IR (KBr) spectrum of **[(**$^{Cy}$**PBP)CoH]**$_2$ (**1**) in $C_6H_6$.

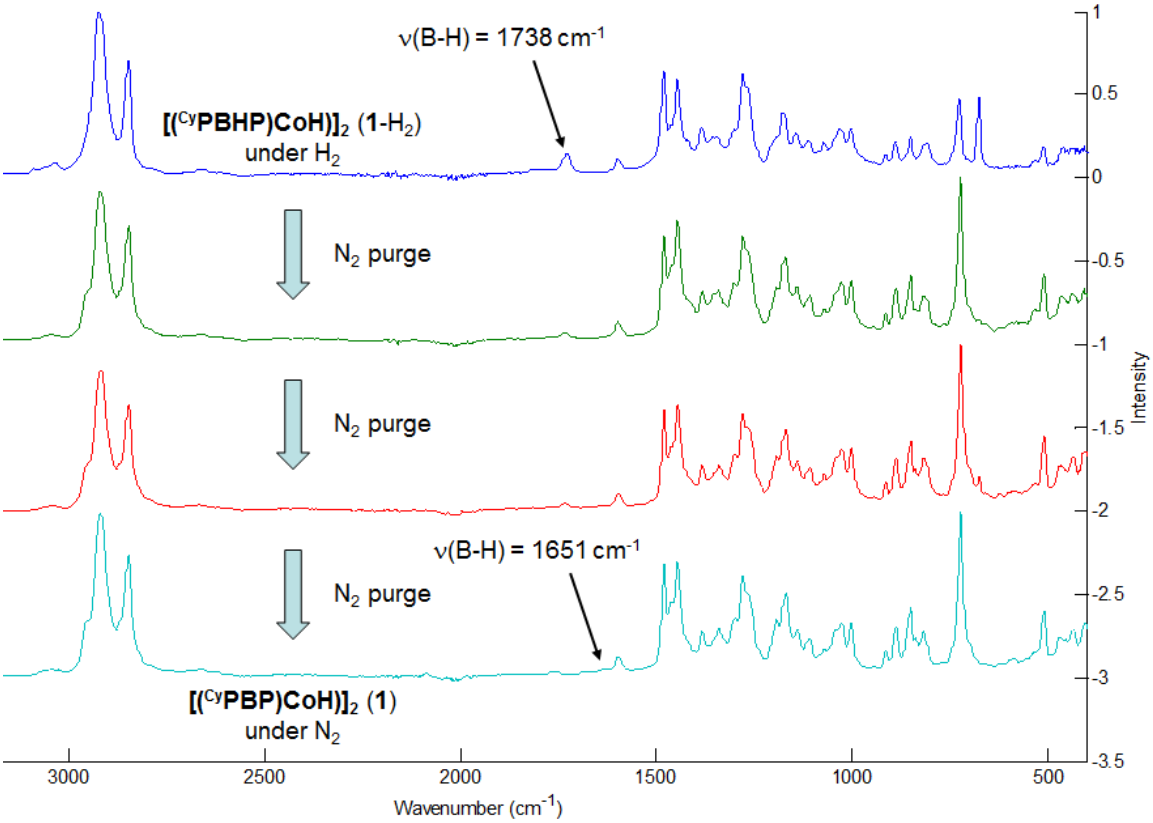


**Figure S14.** Thin film ATR-IR spectrum (blue) of **[(^Cy^PBHP)CoH]$_2$** (**1**-$H_2$) under 1 atm $H_2$. The conversion of **[(^Cy^PBHP)CoH]$_2$** (**1**-$H_2$) to **[(^Cy^PBP)CoH]$_2$** (**1**) was observed by repeatedly dissolving/reforming the thin film using $C_6H_6$ under 1 atm $N_2$.

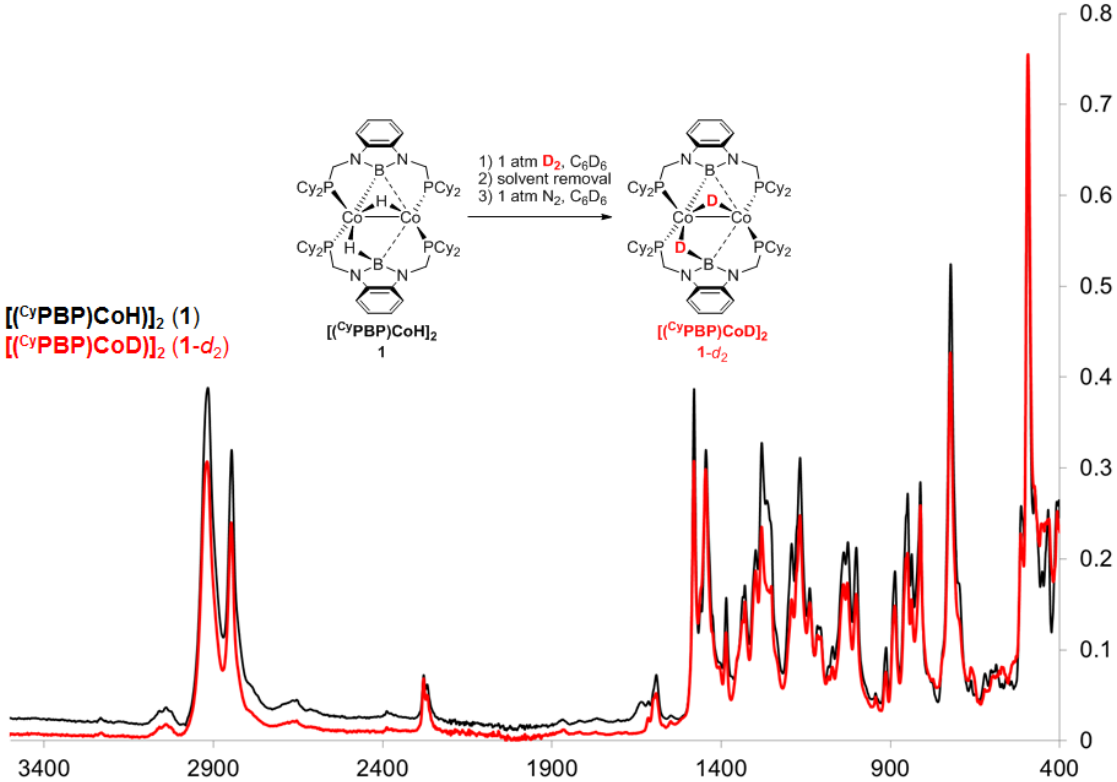


**Figure S15.** Thin film ATR-IR spectra of **[(^Cy^PBP)CoH]$_2$** (**1**, black) and **[(^Cy^PBP)CoD]$_2$** (**1**-$d_2$, red).

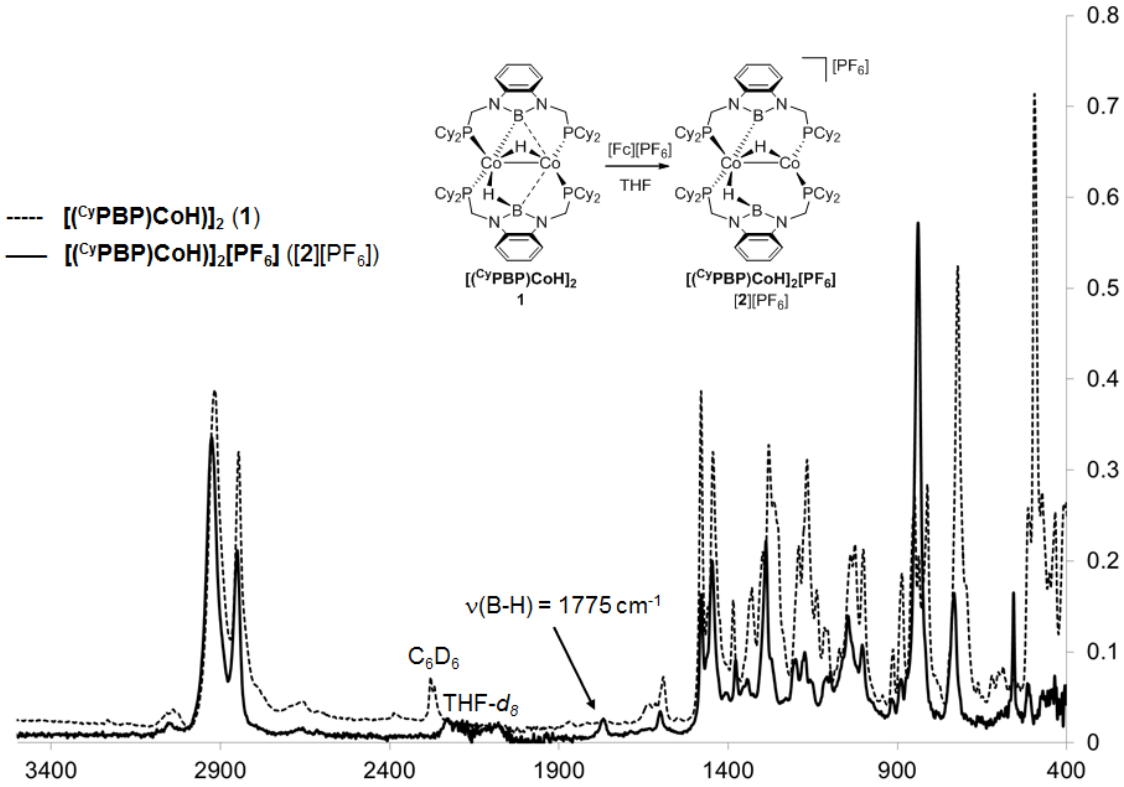


**Figure S16.** Thin film ATR-IR spectra of **[(^Cy^PBP)CoH]$_2$** (**1**, dash trace) and **[(^Cy^PBP)CoH]$_2$[PF$_6$]** ([**2**][PF$_6$], solid trace).

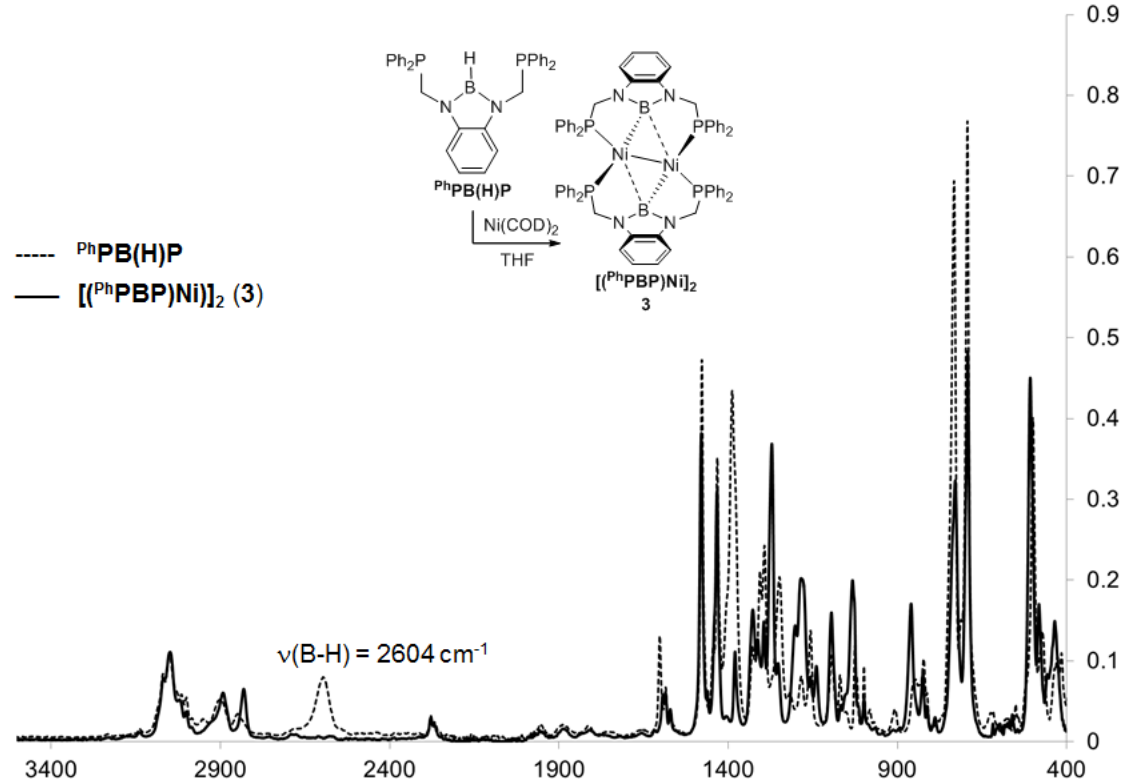


**Figure S17.** Thin film ATR-IR spectra of ligand **^Ph^PB(H)P** (dash trace) and **[(^Ph^PBP)Ni]$_2$** (**3**, solid trace).

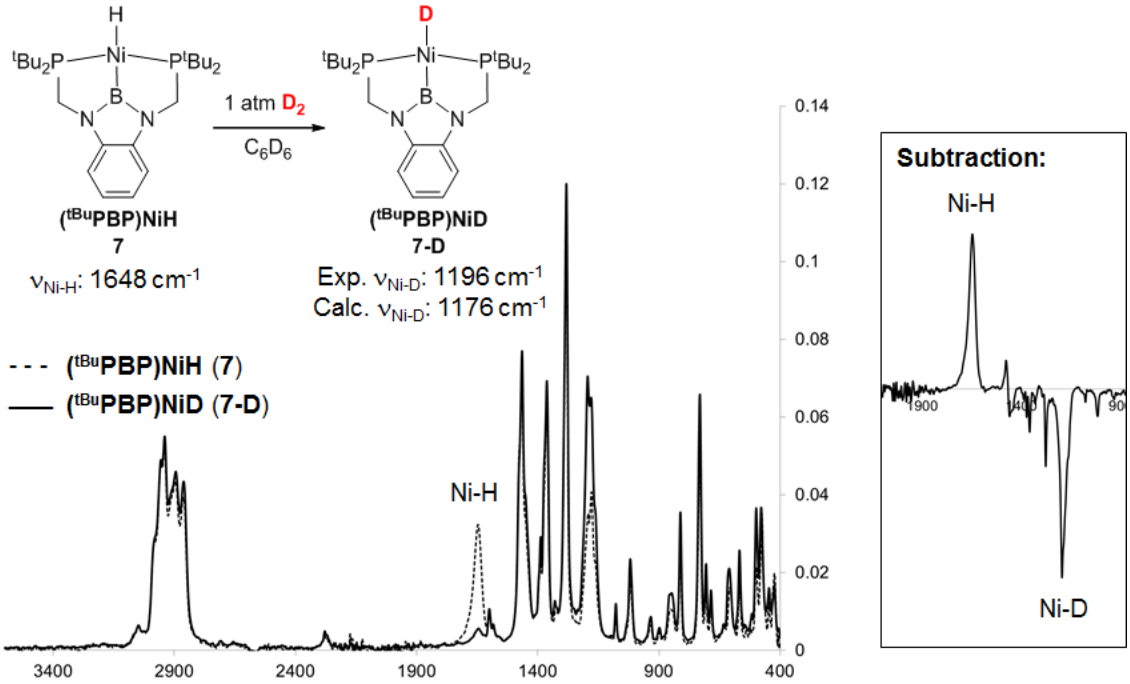


**Figure S18.** Thin film ATR-IR spectra of **($^{tBu}$PBP)NiH** (**7**, dash trace) and **($^{tBu}$PBP)NiD** (**7-D**, solid trace).

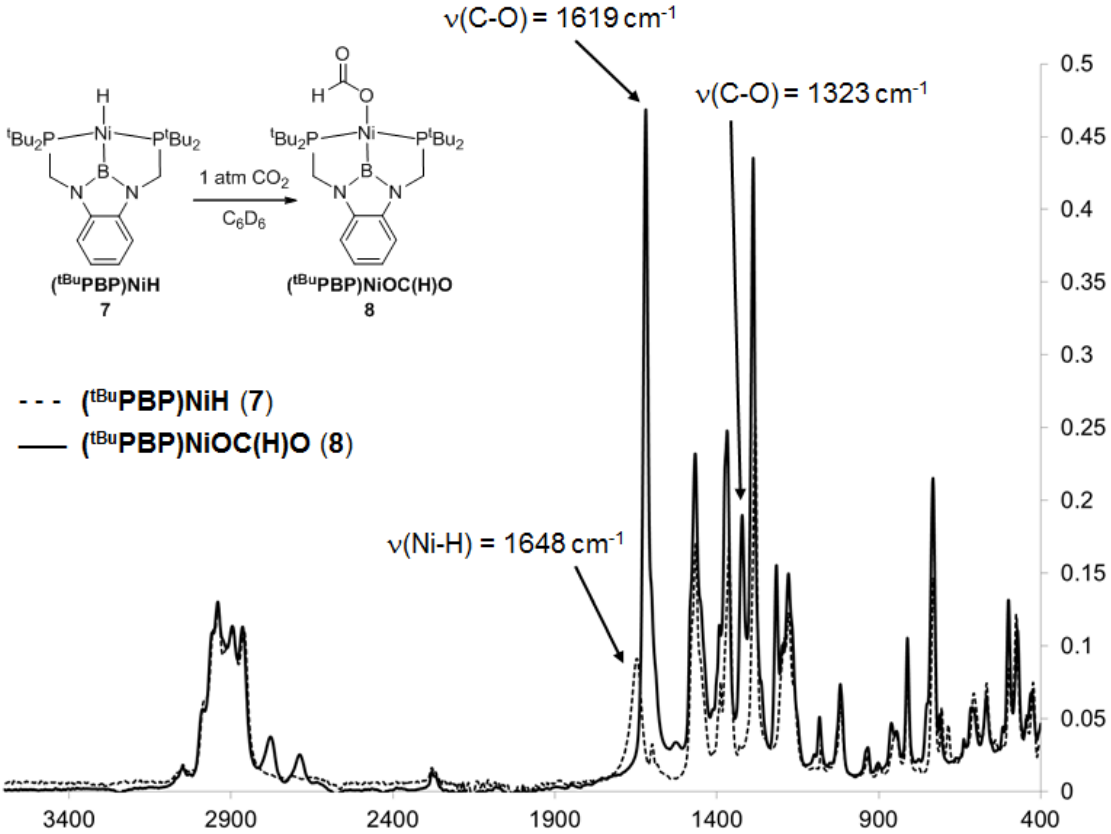


**Figure S19.** Thin film ATR-IR spectra of **($^{tBu}$PBP)NiH** (**7**, dash trace) and **($^{tBu}$PBP)NiOC(H)O** (**8**, solid trace).

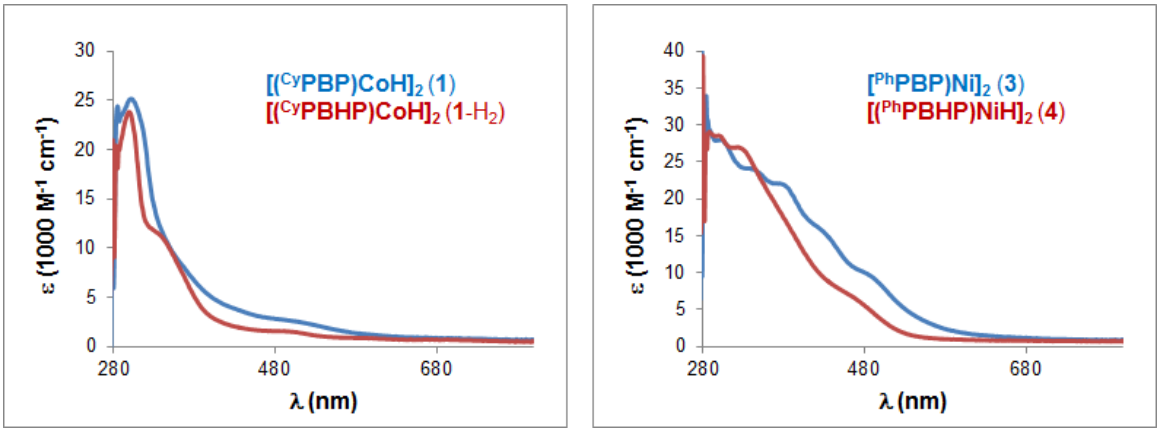


**Figure S20.** Left: UV-vis spectra of **[(^Cy^PBP)CoH]$_2$** (**1**, blue, 3.77 × $10^{-5}$ M, 1 atm $N_2$) and **[(^Cy^PBHP)CoH]$_2$** (**1**-$H_2$, red, 3.77 × $10^{-5}$ M, 1 atm $H_2$) in toluene at 293 K. Right: UV-vis spectra of **[(^Ph^PBP)Ni]$_2$** (**3**, blue, 3.06 × $10^{-5}$ M, 1 atm $N_2$) and **[(^Ph^PBHP)NiH]$_2$** (**4**, red, 3.06 × $10^{-5}$ M, 1 atm $H_2$) in toluene at 293 K.

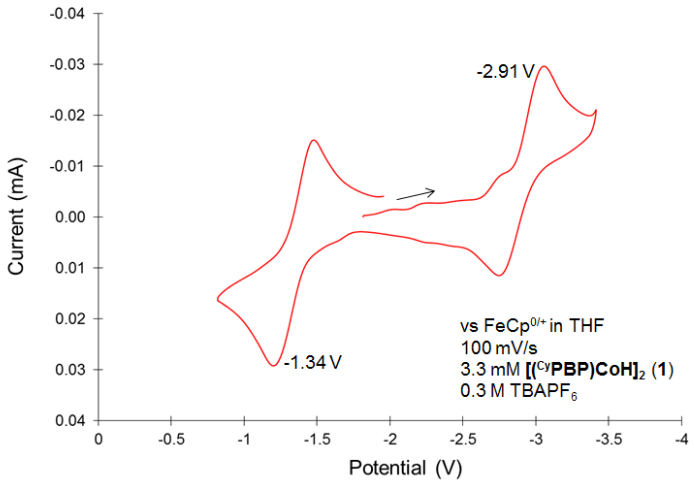


**Figure S21.** The cyclic voltammogram trace acquired for **[(^Cy^PBP)CoH]$_2$** (**1**).

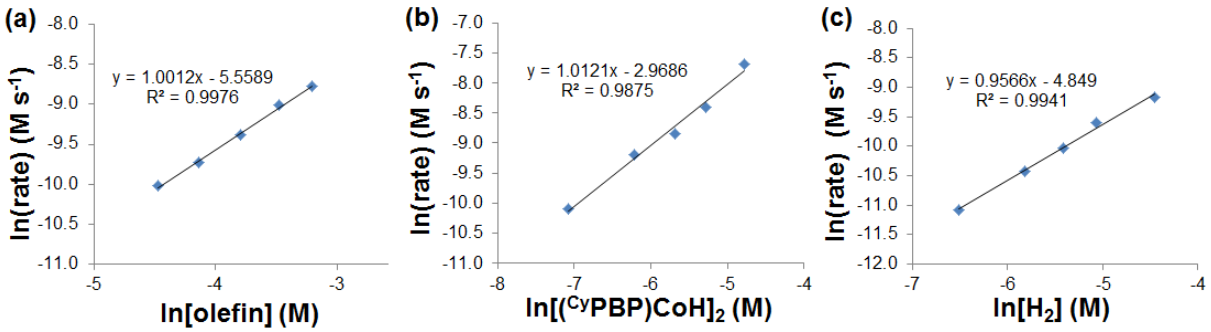


**Figure S22.** Reaction order determination by the method of initial rates for the hydrogenation of *cis*-cyclooctene catalyzed by **[($^{Cy}$PBP)CoH]$_2$** (**1**). (a) Plot of ln(rate) against ln[olefin] ([olefin]: 11.4 – 43.7 mM). (b) Plot of ln(rate) against ln[$Co_2$] ([$Co_2$]: 0.84 – 8.43 mM). (c) Plot of ln(rate) against ln[$H_2$] (pressure of $H_2$: 0.5 – 3.9 atm).

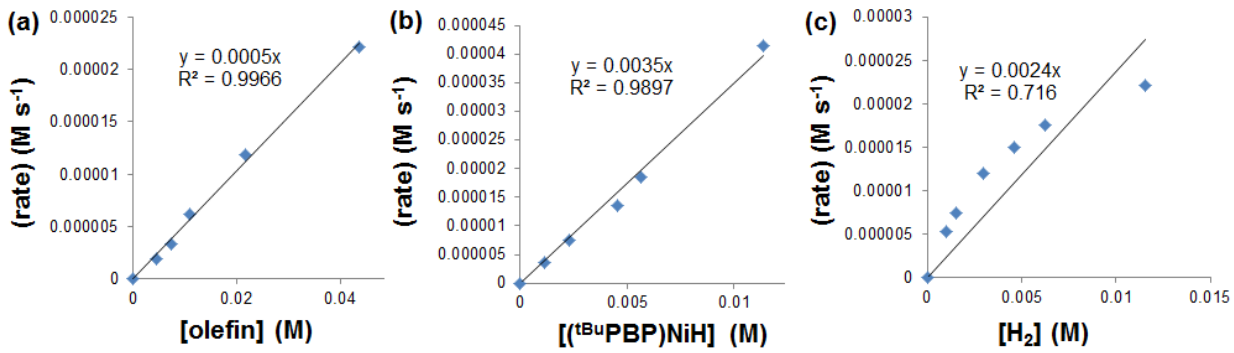


**Figure S23.** Plots of initial rates against the concentrations of olefin, catalyst **($^{tBu}$PBP)NiH** (**7**), and $H_2$ for the hydrogenation of *cis*-cyclooctene catalyzed by complex **7**. (a) Initial rates vs [olefin] (4.36 – 43.6 mM). (b) Initial rates vs [**7**] (1.14 – 11.4 mM). (c) Initial rates vs [$H_2$] (pressure of $H_2$: 0.3 – 3.9 atm).

**Mechanism A**

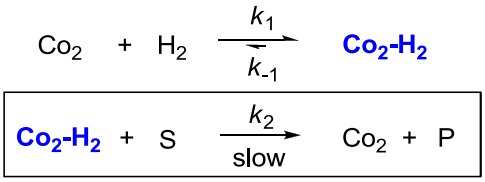


*The solution obtained from the prior equilibrium approximation:*

$$K_{eq1} = \frac{k_1}{k_{-1}} = \frac{[\mathrm{Co_2H_2}]}{[\mathrm{Co_2}][\mathrm{H_2}]}$$

Assuming $Co_2$ and $Co_2$-$H_2$ are rapidly equilibrating:

$$\because [\mathrm{Co_2}] = [\mathrm{Co_2}]_0 - [\mathrm{Co_2H_2}] \therefore K_{eq1} = \frac{[\mathrm{Co_2H_2}]}{([\mathrm{Co_2}]_0 - [\mathrm{Co_2H_2}])[\mathrm{H_2}]} \Rightarrow [\mathrm{Co_2H_2}] = \frac{K_{eq1}[\mathrm{Co_2}]_0[\mathrm{H_2}]}{1 + K_{eq1}[\mathrm{H_2}]}$$

$$v = k_2[\mathrm{Co_2H_2}][\mathrm{S}] = \frac{K_{eq1}k_2[\mathrm{Co_2}]_0[\mathrm{H_2}][\mathrm{S}]}{1 + K_{eq1}[\mathrm{H_2}]}$$

Since $Co_2$-$H_2$ is the resting-state of the catalyst,

$$\frac{[\mathrm{Co_2H_2}]}{[\mathrm{Co_2}]} = K_{eq1}[\mathrm{H_2}] >> 1, \quad v = \frac{K_{eq1}k_2[\mathrm{Co_2}]_0[\mathrm{H_2}][\mathrm{S}]}{1 + K_{eq1}[\mathrm{H_2}]} \approx k_2[\mathrm{Co_2}]_0[\mathrm{S}]$$

**Figure S24.** Rate law derivation for Mechanism **A** (shown in Scheme 2).

**Mechanism B**

$$Co_2 + H_2 \underset{k_{-1}}{\overset{k_1}{\rightleftharpoons}} \mathbf{Co_2\text{-}H_2}$$

$$\mathbf{Co_2\text{-}H_2} + S \underset{k_{-2}}{\overset{k_2}{\rightleftharpoons}} Co_2\text{-}H_2\text{-}S$$

$$Co_2\text{-}H_2\text{-}S + H_2 \xrightarrow[\text{slow}]{k_3} \mathbf{Co_2\text{-}H_2} + P$$

*The solution obtained from the steady-state approximation:*

$$\frac{d[Co_2H_2S]}{dt} = k_2[Co_2H_2][S] - k_{-2}[Co_2H_2S] - k_3[Co_2H_2S][H_2] \approx 0$$

$$[Co_2H_2S] = \frac{k_2[Co_2H_2][S]}{k_{-2} + k_3[H_2]}$$

$$v = k_3[Co_2H_2S][H_2] = \frac{k_2k_3[Co_2H_2][H_2][S]}{k_{-2} + k_3[H_2]}$$

When $k_3$ is rate-limiting, $v \approx \frac{k_2k_3}{k_{-2}}[Co_2H_2][H_2][S]$

Since $Co_2$-$H_2$ is the resting-state of the catalyst, $[Co_2]_0 = [Co_2H_2], v = \frac{k_2k_3}{k_{-2}}[Co_2]_0[H_2][S]$

**Figure S25.** Rate law derivation for Mechanism **B** (shown in Scheme 2).

**Mechanism C**

$$Co_2 + H_2 \underset{k_{-1}}{\overset{k_1}{\rightleftharpoons}} Co_2\text{-}H_2$$

$$0.5\ Co_2\text{-}H_2 \underset{k_{-2}}{\overset{k_2}{\rightleftharpoons}} Co\text{-}H$$

$$Co\text{-}H + S \underset{k_{-3}}{\overset{k_3}{\rightleftharpoons}} Co\text{-}H\text{-}S$$

$$Co\text{-}H\text{-}S + H_2 \xrightarrow[\text{slow}]{k_4} Co\text{-}H + P$$

*The solution obtained from the steady-state approximation:*

$$\frac{d[CoHS]}{dt} = k_3[CoH][S] - k_{-3}[CoHS] - k_4[CoHS][H_2] \approx 0$$

$$[CoHS] = \frac{k_3[CoH][S]}{k_{-3} + k_4[H_2]}$$

$$v = k_4[CoHS][H_2] = \frac{k_3 k_4[CoH][H_2][S]}{k_{-3} + k_4[H_2]}$$

When $k_4$ is rate-limiting, $v \approx \frac{k_3 k_4}{k_{-3}}[CoH][H_2][S]$

Using prior equilibrium approximation, $\frac{[CoH]}{\sqrt{[Co_2H_2]}} = \frac{k_2}{k_{-2}}$, $v = \frac{k_2 k_3 k_4}{k_{-2} k_{-3}}[Co_2H_2]^{\frac{1}{2}}[H_2][S]$

Since $Co_2$-$H_2$ is the resting-state of the catalyst, $[Co_2]_0 = [Co_2H_2], v = \frac{k_2 k_3 k_4}{k_{-2} k_{-3}}[Co_2]_0^{\frac{1}{2}}[H_2][S]$

**Figure S26.** Rate law derivation for Mechanism **C** (shown in Scheme 2).

**Mechanism A**

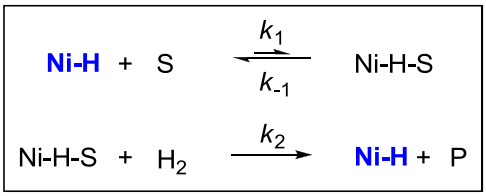


*The solution obtained from the steady-state approximation:*

$$\frac{\mathrm{d[NiHS]}}{\mathrm{dt}} = k_1[\mathrm{NiH}][\mathrm{S}] - k_{-1}[\mathrm{NiHS}] - k_2[\mathrm{NiHS}][\mathrm{H_2}] \approx 0$$

$$[\mathrm{NiHS}] = \frac{k_1[\mathrm{NiH}][\mathrm{S}]}{k_{-1} + k_2[\mathrm{H_2}]}$$

$$v = k_2[\mathrm{NiHS}][\mathrm{H_2}] = \frac{k_1 k_2[\mathrm{NiH}][\mathrm{H_2}][\mathrm{S}]}{k_{-1} + k_2[\mathrm{H_2}]}$$

**Figure S27.** Rate law derivation for Mechanism **A** (shown in Scheme 5).

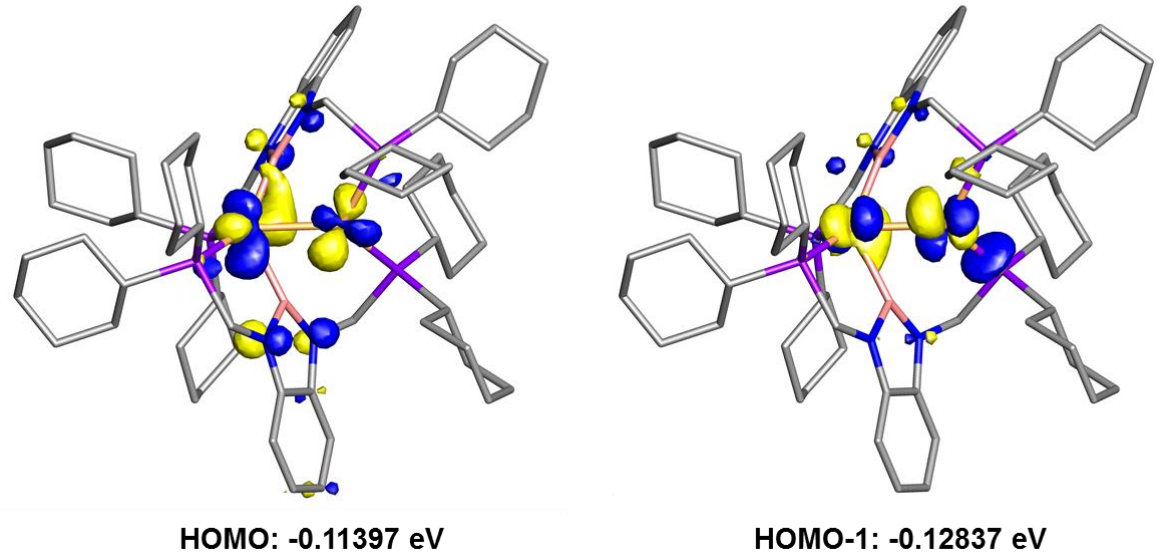


**Figure S28.** The two singly occupied molecular orbitals (isovalue = 0.05) of complex **[($^{Cy}$PBP)CoH]$_2$** (**1**). Hydrogenation atoms are omitted for clarity.

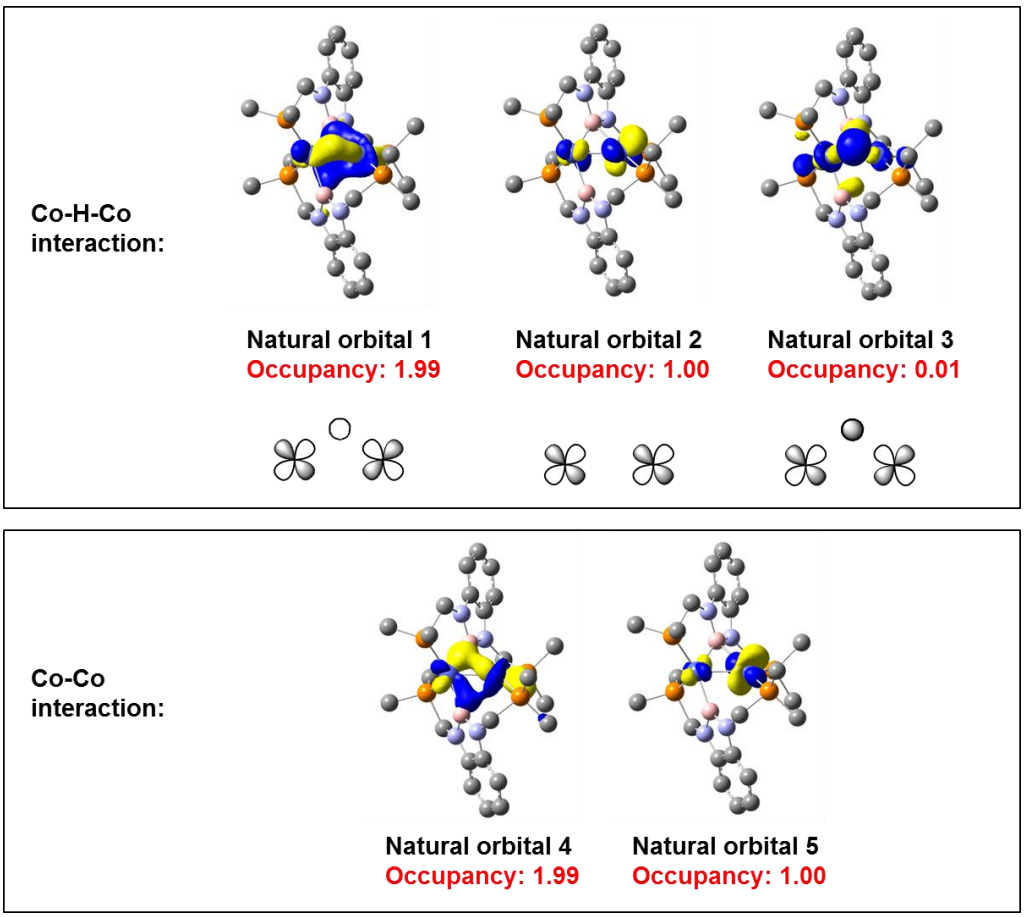


**Figure S29.** Five natural orbitals (NOs, isovalue = 0.05) illustrating the electronic structure and the predicted $S = 1$ spin state of model complex **[($^{Me}$PBP)CoH]$_2$** ([**1'**]). The rest of the NOs (not shown) have occupancy of > 1.99 or < 0.01. Three NOs that are associated with the Co-H-Co core are NO 1-3. These orbitals are in-phase (NO 1, occupancy: 1.99), non-bonding (NO 2, occupancy: 1.00), and out-of-phase (NO 3, occupancy: 0.01) combinations of two d(Co) and one s(H) orbitals. In addition, we found a π(Co-Co) (NO 4, occupancy: 1.99) and a π*(Co-Co) (NO 5, occupancy: 1.00) orbitals. Taken collectively, the orbital occupancies of NO 2, NO 4, and NO 5 indicate the absence of a net Co-Co bond. In turn, the two Co atoms are involved in a 3c-2e interaction (NO 1) through the bridging hydride. The NO analysis also reveals that the two unpaired electrons are aligned ferromagnetically in two orthogonal π*(Co-Co) orbitals (NO 2, NO 5), leading to an $S = 1$ configuration which is in agreement with the spin-density plot shown in Figure 1.

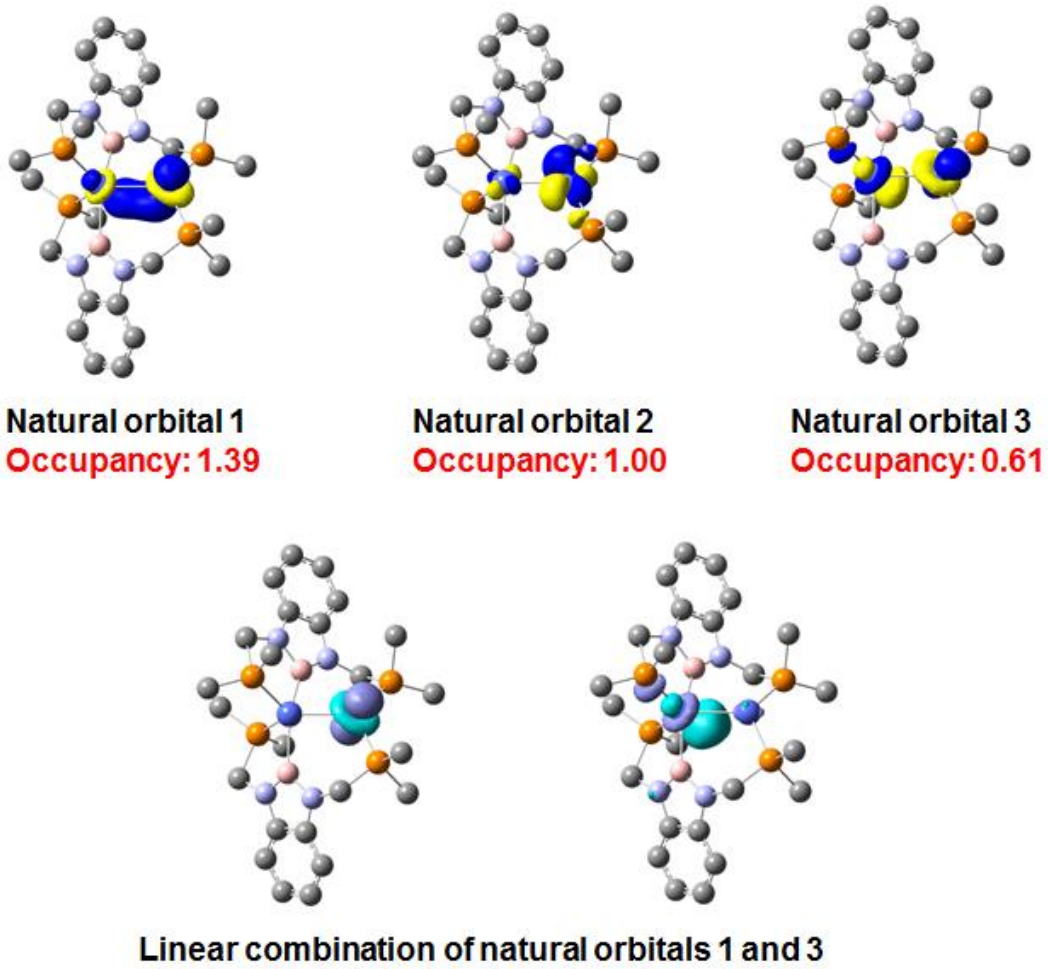


**Figure S30.** Top: Three natural orbitals (NOs, isovalue = 0.05) illustrating the electronic structure and the predicted $S$ = ½ spin state of model complex **[(**$^{Me}$**PBP)CoH]**$_2^+$ ([**2'**]$^+$). The rest of the NOs (not shown) have occupancy of > 1.99 or < 0.01. Examinations of NO 1 and NO 3 reveal that they are, respectively, symmetry related Co-Co bonding and antibonding orbitals. These results are in line with two Co being antiferromagnetically coupled (a strongly antiferromagnetically coupled system would have occupancies of 1.00/1.00 whereas a fully electronically paired system would have occupancies of 2/0). Taking linear combinations of NO 1 and NO 3 recovers two localized Co d-orbitals (Bottom). These orbitals are magnetic natural orbitals (MNOs) which could be employed to visualize magnetic interactions (also see ref 22). According to these calculations, the two Co in complex [**2**]$^+$ could be described as antiferromagnetically coupled. The unpaired electron is localized in NO 2 which has a large contribution from Co2, consistent with the experimentally obtained EPR spectrum showing hyperfine coupling to only one Co atom.

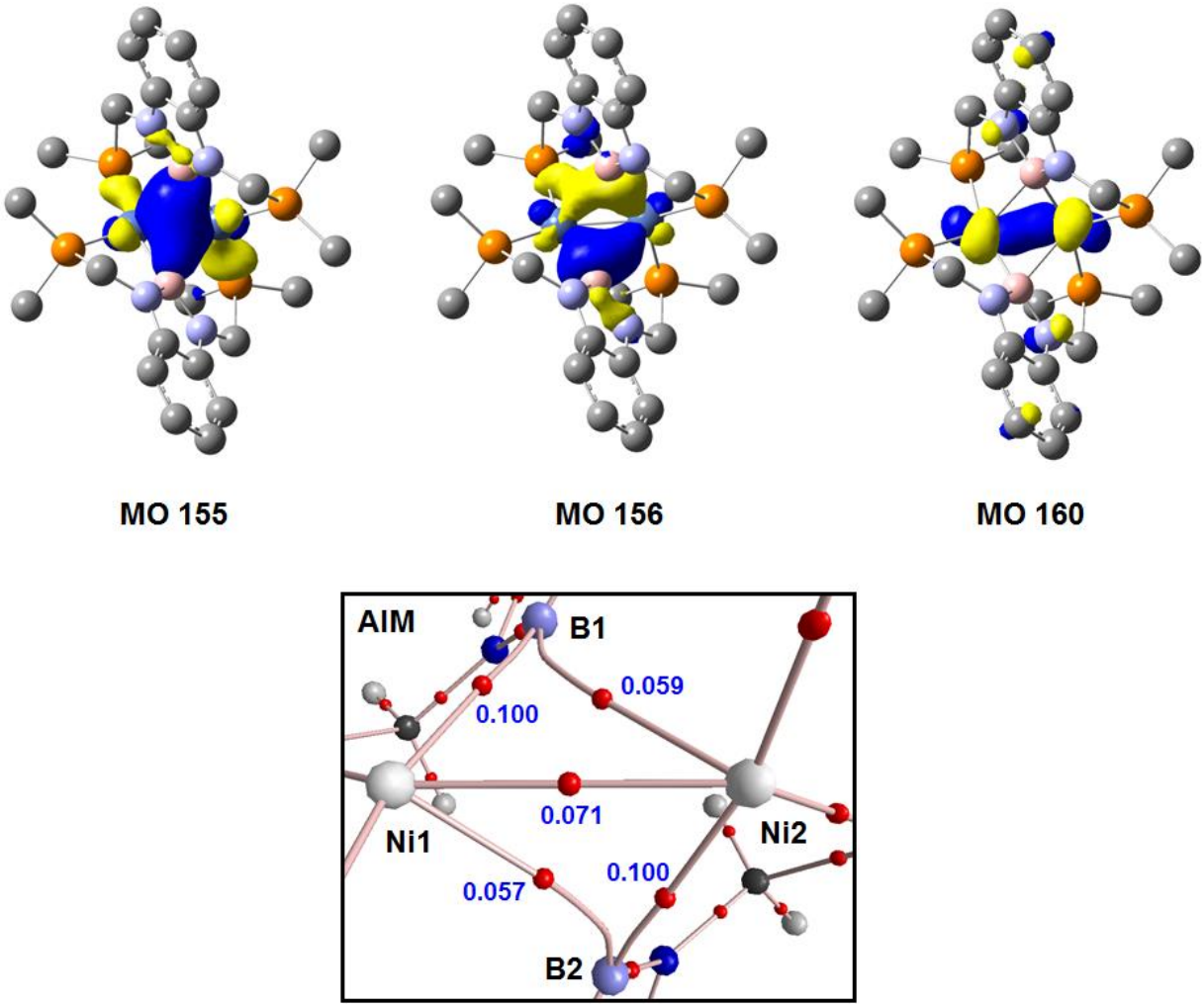


**Figure S31.** Top: Molecular orbitals (isovalue = 0.05) of complex **[(^Me^PBP)Ni]$_2$** (**3'**) showing the Ni-($\mu_2$-B)$_2$-Ni 4c-4e interaction (MO 155, MO 156) as well as the σ(Ni-Ni) orbital (MO 160). Hydrogen atoms are omitted for clarity. Bottom: Calculated electron density plot for **3'** with bond paths (pink), (3,-1) bond critical points (BCPs, red), and electron density (e bohr$^{-3}$, blue).

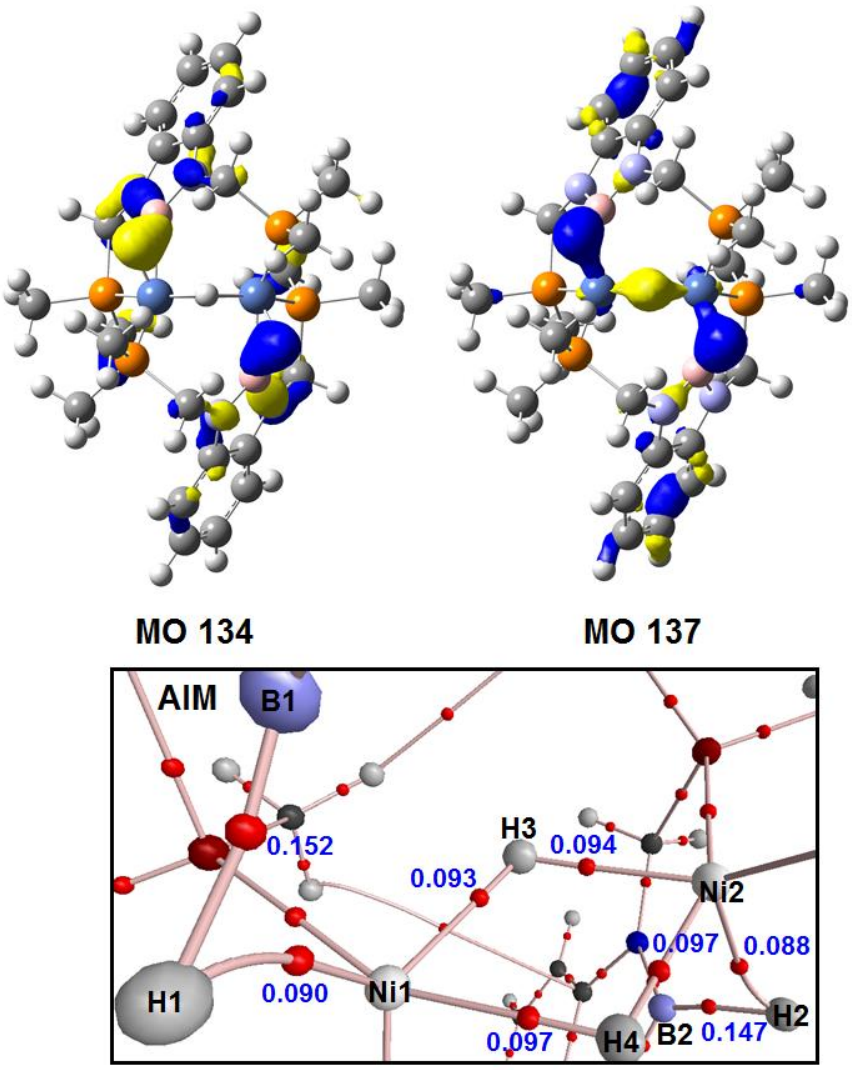


**Figure S32.** Top: Molecular orbitals (isovalue = 0.05) of complex **[($^{Me}$PBHP)NiH]$_2$** (**4'**) showing the agostic σ-borane coordination mode (MO 134, MO 137). Hydrogen atoms are omitted for clarity. Bottom: Calculated electron density plot for **4'** with bond paths (pink), (3,-1) bond critical points (BCPs, red), and electron density (e bohr$^{-3}$, blue). The absence of a bond path/BCP between B1-Ni1 and B2-Ni2 suggests that the coordination mode of the borane ligand is closer to *pseudo* agostic.

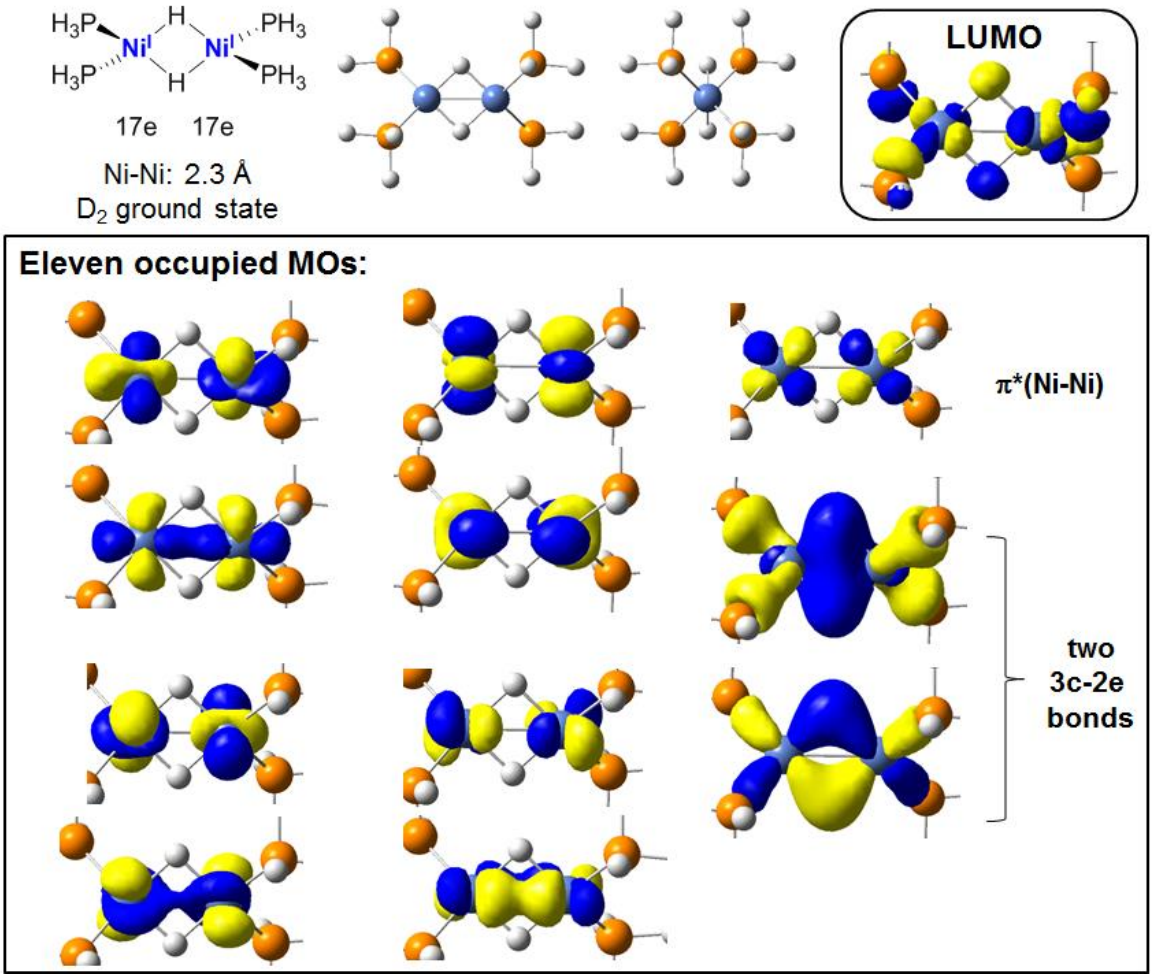


**Figure S33.** Geometry of $(PH_3)_2Ni$-($\mu_2$-H)$_2$-$Ni(PH_3)_2$ optimized at BP86/6-31g(d) level of theory by DFT. The MOs (isovalue = 0.05) illustrate the three-center-two-electron bonds as well as the presence of a π*(Ni-Ni) bond. Hydrogen atoms are omitted for clarity.

**Table S1.** Calculated EPR parameters for complex **[($^{Me}$PBP)CoH]$_2^+$** ([**2'**]$^+$) at BP86/6-31+g(d,p) level of theory.

| Atom | Calculated coupling constant (MHz) |
|---|---|
| Co | [28, 5, 23] |
| Co | [233, 97, 136] |
| P | [43, 20, 22] |
| P | [20, 6, 26] |
| P | [4, 1, 5] |
| P | [13, 9, 22] |

**DFT structural coordinates**

**[($^{Me}$PBHP)Co] (1')**

| | | | |
|---|---|---|---|
| Co | 0.227000 | 1.283000 | 0.373000 |
| Co | -0.270000 | -0.991000 | 0.724000 |
| P | -1.943000 | -1.584000 | 2.164000 |
| P | 1.694000 | 2.272000 | 1.724000 |
| P | 0.120000 | -2.535000 | -0.831000 |
| P | 0.144000 | 2.177000 | -1.668000 |
| N | 2.995000 | 0.194000 | 0.652000 |
| N | -2.915000 | 0.523000 | 0.820000 |
| N | -2.301000 | 1.261000 | -1.246000 |
| N | 2.192000 | -0.904000 | -1.178000 |
| C | -3.612000 | 0.842000 | -1.320000 |
| C | 5.401000 | -0.531000 | 0.388000 |
| H | 5.730000 | -0.094000 | 1.165000 |
| C | -1.480000 | 1.597000 | -2.373000 |
| H | -1.903000 | 2.315000 | -2.908000 |
| H | -1.344000 | 0.806000 | -2.954000 |
| B | 1.744000 | -0.019000 | -0.077000 |
| C | -4.005000 | 0.389000 | -0.036000 |
| C | 4.058000 | -0.460000 | 0.052000 |
| C | -4.488000 | 0.786000 | -2.395000 |
| H | -4.221000 | 1.076000 | -3.260000 |
| C | 6.262000 | -1.263000 | -0.444000 |
| H | 7.185000 | -1.325000 | -0.226000 |
| C | 3.563000 | -1.133000 | -1.091000 |
| C | 3.133000 | 1.076000 | 1.789000 |
| H | 3.992000 | 1.566000 | 1.743000 |
| H | 3.111000 | 0.557000 | 2.633000 |
| C | 4.425000 | -1.842000 | -1.916000 |
| H | 4.101000 | -2.281000 | -2.693000 |
| C | -6.167000 | -0.130000 | -0.918000 |
| H | -7.050000 | -0.453000 | -0.791000 |
| C | 5.781000 | -1.895000 | -1.578000 |
| H | 6.383000 | -2.373000 | -2.137000 |
| B | -1.739000 | 1.009000 | 0.082000 |
| C | -5.290000 | -0.090000 | 0.170000 |
| H | -5.568000 | -0.383000 | 1.030000 |
| C | -2.884000 | 0.023000 | 2.176000 |
| H | -3.805000 | -0.123000 | 2.507000 |
| H | -2.437000 | 0.676000 | 2.770000 |
| C | -5.775000 | 0.289000 | -2.172000 |
| H | -6.390000 | 0.240000 | -2.895000 |
| C | 1.314000 | -1.731000 | -1.993000 |
| H | 1.838000 | -2.416000 | -2.480000 |
| H | 0.831000 | -1.174000 | -2.654000 |
| H | 0.084000 | 0.381000 | 1.567000 |
| H | -1.098000 | 2.028000 | 0.719000 |
| C | 1.287000 | 1.691000 | -2.998000 |
| H | 2.292000 | 1.718000 | -2.632000 |
| H | 1.053000 | 0.700000 | -3.325000 |
| H | 1.189000 | 2.371000 | -3.819000 |
| C | -0.050000 | 3.983000 | -1.773000 |
| H | 0.909000 | 4.451000 | -1.687000 |
| H | -0.490000 | 4.241000 | -2.714000 |
| H | -0.683000 | 4.321000 | -0.979000 |
| C | 2.592000 | 3.842000 | 1.516000 |
| H | 1.899000 | 4.656000 | 1.549000 |
| H | 3.308000 | 3.950000 | 2.304000 |
| H | 3.096000 | 3.841000 | 0.573000 |
| C | 1.262000 | 2.305000 | 3.492000 |
| H | 1.996000 | 2.870000 | 4.028000 |
| H | 0.302000 | 2.759000 | 3.616000 |
| H | 1.236000 | 1.305000 | 3.872000 |
| C | 1.026000 | -3.954000 | -0.140000 |
| H | 0.330000 | -4.683000 | 0.217000 |
| H | 1.641000 | -4.389000 | -0.900000 |
| H | 1.642000 | -3.623000 | 0.670000 |
| C | -1.137000 | -3.259000 | -1.931000 |
| H | -0.704000 | -4.063000 | -2.488000 |
| H | -1.953000 | -3.629000 | -1.346000 |
| H | -1.494000 | -2.510000 | -2.607000 |
| C | -1.643000 | -1.854000 | 3.939000 |
| H | -2.498000 | -2.322000 | 4.378000 |
| H | -0.787000 | -2.484000 | 4.064000 |
| H | -1.466000 | -0.913000 | 4.418000 |
| C | -3.308000 | -2.702000 | 1.718000 |
| H | -3.047000 | -3.706000 | 1.979000 |
| H | -4.192000 | -2.414000 | 2.248000 |
| H | -3.488000 | -2.642000 | 0.665000 |

**[($^{Me}$PBHP)CoH]$^{+}$** ([**2'**]$^{+}$)

| | | | | | | | |
|---|---|---|---|---|---|---|---|
| Co | 0.160000 | 1.707000 | 0.538000 | H | -3.507000 | -2.066000 | 2.182000 |
| Co | -0.031000 | -0.765000 | 0.546000 | B | 2.217000 | -0.903000 | 0.510000 |
| P | 0.164000 | -2.227000 | -1.132000 | C | -6.476000 | -0.662000 | -0.699000 |
| P | 2.195000 | 2.563000 | 0.987000 | H | -7.372000 | -0.960000 | -0.585000 |
| P | -1.320000 | 2.888000 | -0.683000 | B | -1.868000 | -0.364000 | -0.092000 |
| P | -1.122000 | -1.854000 | 2.141000 | H | -0.120000 | 0.323000 | 1.432000 |
| N | 2.672000 | -1.901000 | -0.410000 | H | 1.377000 | -1.066000 | 1.328000 |
| N | 3.297000 | 0.017000 | 0.675000 | C | 3.093000 | 3.426000 | -0.341000 |
| N | -2.510000 | 0.478000 | -1.094000 | H | 2.674000 | 4.401000 | -0.479000 |
| N | -2.970000 | -1.115000 | 0.474000 | H | 4.125000 | 3.516000 | -0.074000 |
| C | 1.858000 | -2.971000 | -0.968000 | H | 3.007000 | 2.869000 | -1.250000 |
| H | 1.842000 | -3.756000 | -0.362000 | C | 2.313000 | 3.673000 | 2.424000 |
| H | 2.205000 | -3.253000 | -1.850000 | H | 3.333000 | 3.957000 | 2.574000 |
| C | 4.356000 | -0.403000 | -0.138000 | H | 1.721000 | 4.547000 | 2.249000 |
| C | 3.347000 | 1.201000 | 1.525000 | H | 1.952000 | 3.167000 | 3.296000 |
| H | 4.274000 | 1.550000 | 1.531000 | C | -1.071000 | 4.303000 | -1.800000 |
| H | 3.118000 | 0.939000 | 2.452000 | H | -2.008000 | 4.583000 | -2.235000 |
| C | 3.960000 | -1.576000 | -0.824000 | H | -0.674000 | 5.129000 | -1.248000 |
| C | -3.891000 | 0.234000 | -1.086000 | H | -0.386000 | 4.030000 | -2.575000 |
| C | -4.169000 | -0.768000 | -0.141000 | C | -2.803000 | 3.275000 | 0.298000 |
| C | 5.614000 | 0.139000 | -0.360000 | H | -2.656000 | 4.199000 | 0.819000 |
| H | 5.904000 | 0.907000 | 0.115000 | H | -3.648000 | 3.364000 | -0.352000 |
| C | -1.964000 | 1.595000 | -1.851000 | H | -2.978000 | 2.491000 | 1.005000 |
| H | -2.668000 | 1.984000 | -2.426000 | C | 0.214000 | -1.529000 | -2.812000 |
| H | -1.229000 | 1.275000 | -2.433000 | H | 0.729000 | -2.204000 | -3.463000 |
| C | 6.040000 | -1.620000 | -1.985000 | H | -0.785000 | -1.383000 | -3.167000 |
| H | 6.623000 | -2.011000 | -2.624000 | H | 0.727000 | -0.591000 | -2.794000 |
| C | 6.439000 | -0.477000 | -1.297000 | C | -1.001000 | -3.621000 | -1.229000 |
| H | 7.296000 | -0.108000 | -1.473000 | H | -1.080000 | -4.088000 | -0.269000 |
| C | 4.792000 | -2.192000 | -1.744000 | H | -1.963000 | -3.262000 | -1.531000 |
| H | 4.520000 | -2.982000 | -2.198000 | H | -0.646000 | -4.334000 | -1.944000 |
| C | -5.455000 | -1.245000 | 0.058000 | C | -0.590000 | -3.419000 | 2.904000 |
| H | -5.635000 | -1.938000 | 0.683000 | H | 0.383000 | -3.295000 | 3.331000 |
| C | -4.913000 | 0.810000 | -1.830000 | H | -1.284000 | -3.695000 | 3.671000 |
| H | -4.736000 | 1.496000 | -2.463000 | H | -0.558000 | -4.186000 | 2.159000 |
| C | -6.199000 | 0.344000 | -1.610000 | C | -1.478000 | -0.887000 | 3.641000 |
| H | -6.916000 | 0.729000 | -2.102000 | H | -2.075000 | -1.472000 | 4.309000 |
| C | -2.822000 | -2.154000 | 1.471000 | H | -0.559000 | -0.624000 | 4.122000 |
| H | -2.892000 | -3.053000 | 1.063000 | H | -2.009000 | 0.003000 | 3.374000 |

**[($^{Me}$PBP)Ni] (3')**

| | | | |
|---|---|---|---|
| Ni | 0.176000 | -1.280000 | 0.706000 |
| Ni | -0.176000 | 0.928000 | 1.116000 |
| P | 1.881000 | -1.592000 | 2.029000 |
| P | -1.866000 | 0.724000 | 2.479000 |
| P | 0.048000 | -2.797000 | -0.822000 |
| P | -0.065000 | 2.903000 | 0.257000 |
| C | -3.308000 | 0.592000 | 1.288000 |
| H | -4.146000 | -0.010000 | 1.700000 |
| H | -3.689000 | 1.621000 | 1.124000 |
| C | -3.600000 | -0.058000 | -1.091000 |
| N | -1.544000 | -0.873000 | -1.665000 |
| C | 3.605000 | 0.466000 | -1.001000 |
| N | 2.801000 | -0.037000 | 0.026000 |
| C | 3.316000 | -1.015000 | 0.971000 |
| H | 4.149000 | -0.598000 | 1.577000 |
| H | 3.711000 | -1.907000 | 0.442000 |
| N | 1.553000 | 1.441000 | -1.226000 |
| C | -0.584000 | -1.774000 | -2.285000 |
| H | 0.265000 | -1.238000 | -2.751000 |
| H | -1.068000 | -2.406000 | -3.053000 |
| C | 4.757000 | 1.795000 | -3.182000 |
| H | 5.218000 | 2.308000 | -4.032000 |
| C | 2.833000 | 1.390000 | -1.773000 |
| H | -3.469000 | 1.792000 | 4.080000 |
| H | -1.759000 | 2.172000 | 4.466000 |
| H | -2.562000 | 3.006000 | 3.109000 |
| C | -2.077000 | -0.777000 | 3.565000 |
| H | -1.296000 | -0.776000 | 4.343000 |
| H | -3.069000 | -0.805000 | 4.051000 |
| H | -1.935000 | -1.673000 | 2.938000 |
| C | 2.107000 | -0.626000 | 3.608000 |
| H | 1.333000 | -0.926000 | 4.334000 |
| H | 3.103000 | -0.794000 | 4.056000 |
| H | 1.970000 | 0.444000 | 3.383000 |
| C | 2.509000 | -3.258000 | 2.598000 |
| H | 3.490000 | -3.183000 | 3.100000 |
| H | 1.783000 | -3.696000 | 3.303000 |
| H | 2.594000 | -3.936000 | 1.733000 |
| C | 1.522000 | -3.675000 | -1.561000 |
| H | 1.895000 | -4.437000 | -0.857000 |
| H | 1.258000 | -4.174000 | -2.511000 |
| H | 2.327000 | -2.946000 | -1.749000 |
| C | -1.203000 | -4.185000 | -0.804000 |
| H | -1.219000 | -4.733000 | -1.764000 |
| H | -0.963000 | -4.888000 | 0.011000 |
| H | -2.202000 | -3.762000 | -0.611000 |
| B | 1.433000 | 0.541000 | -0.045000 |
| N | -2.797000 | 0.026000 | 0.050000 |
| C | -3.400000 | -0.837000 | -3.416000 |
| H | -2.813000 | -1.263000 | -4.236000 |
| C | -4.939000 | 0.309000 | -1.296000 |
| H | -5.535000 | 0.742000 | -0.485000 |
| C | -2.826000 | -0.625000 | -2.152000 |
| C | 5.514000 | 0.879000 | -2.426000 |
| H | 6.558000 | 0.687000 | -2.693000 |
| B | -1.428000 | -0.482000 | -0.233000 |
| C | 3.406000 | 2.057000 | -2.867000 |
| H | 2.819000 | 2.757000 | -3.471000 |
| C | -4.750000 | -0.477000 | -3.611000 |
| H | -5.211000 | -0.636000 | -4.592000 |
| C | 4.944000 | 0.202000 | -1.326000 |
| H | 5.540000 | -0.502000 | -0.736000 |
| C | -5.508000 | 0.091000 | -2.569000 |
| H | -6.552000 | 0.370000 | -2.746000 |
| C | 0.592000 | 2.505000 | -1.473000 |
| H | -0.251000 | 2.177000 | -2.112000 |
| H | 1.077000 | 3.379000 | -1.947000 |
| C | 1.146000 | 4.209000 | 0.818000 |
| H | 1.163000 | 5.077000 | 0.136000 |
| H | 0.874000 | 4.549000 | 1.831000 |
| H | 2.151000 | 3.760000 | 0.863000 |
| C | -1.565000 | 3.948000 | -0.121000 |
| H | -1.974000 | 4.365000 | 0.815000 |
| H | -1.320000 | 4.783000 | -0.801000 |
| H | -2.338000 | 3.317000 | -0.589000 |
| C | -2.485000 | 2.047000 | 3.646000 |

**[($^{Me}$PBHP)NiH] (4')**

| | | | |
|---|---|---|---|
| Ni | 0.134000 | -1.310000 | 0.555000 |
| Ni | -0.137000 | 1.307000 | 0.550000 |
| P | 1.869000 | -1.770000 | 1.837000 |
| P | -1.868000 | 1.774000 | 1.831000 |
| P | 0.116000 | -2.534000 | -1.275000 |
| P | -0.115000 | 2.534000 | -1.276000 |
| C | -2.906000 | 0.214000 | 2.193000 |
| H | -2.353000 | -0.330000 | 2.981000 |
| H | -3.896000 | 0.487000 | 2.601000 |
| C | -4.090000 | -0.591000 | 0.121000 |
| N | -2.494000 | -1.964000 | -0.794000 |
| C | 4.089000 | 0.589000 | 0.120000 |
| N | 3.034000 | 0.650000 | 1.041000 |
| C | 2.908000 | -0.209000 | 2.196000 |
| H | 2.357000 | 0.335000 | 2.984000 |
| H | 3.898000 | -0.483000 | 2.604000 |
| N | 2.499000 | 1.976000 | -0.787000 |
| C | -1.704000 | -2.603000 | -1.831000 |
| H | -1.808000 | -2.051000 | -2.787000 |
| H | -2.014000 | -3.651000 | -2.015000 |
| C | 5.869000 | 0.843000 | -2.037000 |
| H | 6.572000 | 0.934000 | -2.871000 |
| C | 3.758000 | 1.413000 | -1.004000 |
| B | 1.957000 | 1.462000 | 0.477000 |
| N | -3.031000 | -0.644000 | 1.037000 |
| C | -4.647000 | -1.546000 | -2.081000 |
| H | -4.397000 | -2.177000 | -2.940000 |
| C | -5.318000 | 0.085000 | 0.167000 |
| H | -5.586000 | 0.713000 | 1.023000 |
| C | -3.758000 | -1.413000 | -1.004000 |
| C | 6.199000 | 0.041000 | -0.929000 |
| H | 7.158000 | -0.488000 | -0.907000 |
| B | -1.948000 | -1.448000 | 0.467000 |
| C | 4.642000 | 1.540000 | -2.086000 |
| H | 4.393000 | 2.173000 | -2.943000 |
| C | -5.878000 | -0.858000 | -2.027000 |
| H | -6.585000 | -0.955000 | -2.858000 |
| C | 5.312000 | -0.096000 | 0.160000 |
| H | 5.580000 | -0.726000 | 1.015000 |
| C | -6.210000 | -0.058000 | -0.918000 |
| H | -7.172000 | 0.463000 | -0.892000 |
| C | 1.706000 | 2.609000 | -1.827000 |
| H | 1.815000 | 2.054000 | -2.781000 |
| H | 2.012000 | 3.657000 | -2.014000 |
| C | 0.535000 | -4.353000 | -1.224000 |
| H | 0.268000 | -4.865000 | -2.165000 |
| H | 1.616000 | -4.477000 | -1.048000 |
| H | -0.009000 | -4.823000 | -0.389000 |
| C | 0.986000 | -2.047000 | -2.849000 |
| H | 2.075000 | -2.078000 | -2.683000 |
| H | 0.728000 | -2.712000 | -3.693000 |
| H | 0.715000 | -1.010000 | -3.103000 |
| C | 3.197000 | -2.990000 | 1.340000 |
| H | 4.014000 | -3.027000 | 2.082000 |
| H | 2.754000 | -3.996000 | 1.255000 |
| H | 3.616000 | -2.706000 | 0.361000 |
| C | 1.585000 | -2.333000 | 3.595000 |
| H | 1.131000 | -3.338000 | 3.584000 |
| H | 2.523000 | -2.370000 | 4.179000 |
| H | 0.877000 | -1.646000 | 4.087000 |
| C | -0.538000 | 4.352000 | -1.224000 |
| H | -0.268000 | 4.865000 | -2.165000 |
| H | -1.619000 | 4.475000 | -1.053000 |
| H | 0.003000 | 4.823000 | -0.387000 |
| C | -0.979000 | 2.048000 | -2.854000 |
| H | -2.068000 | 2.081000 | -2.692000 |
| H | -0.717000 | 2.712000 | -3.697000 |
| H | -0.709000 | 1.011000 | -3.107000 |
| C | -3.194000 | 2.991000 | 1.327000 |
| H | -3.613000 | 2.702000 | 0.350000 |
| H | -4.012000 | 3.031000 | 2.070000 |
| H | -2.752000 | 3.998000 | 1.238000 |
| C | -1.582000 | 2.344000 | 3.587000 |
| H | -1.125000 | 3.348000 | 3.571000 |
| H | -2.521000 | 2.387000 | 4.169000 |
| H | -0.877000 | 1.657000 | 4.082000 |
| H | -1.150000 | -2.080000 | 1.270000 |
| H | 1.151000 | 2.081000 | 1.273000 |
| H | -0.016000 | -0.002000 | 1.496000 |
| H | 0.071000 | 0.006000 | -0.405000 |

**$(PH_3)_2Ni\text{-}(\mu_2\text{-}H)_2\text{-}Ni(PH_3)_2$**

| | | | | | | | |
|---|---|---|---|---|---|---|---|
| Ni | -1.148000 | -0.000000 | -0.000000 | P | 2.384000 | -1.211000 | -1.189000 |
| Ni | 1.148000 | -0.000000 | 0.000000 | H | 3.816000 | -1.094000 | -1.209000 |
| P | -2.383000 | -1.204000 | 1.195000 | H | 2.371000 | -2.643000 | -1.098000 |
| H | -2.364000 | -2.637000 | 1.121000 | H | 2.232000 | -1.165000 | -2.615000 |
| H | -2.239000 | -1.142000 | 2.622000 | P | 2.383000 | 1.211000 | 1.189000 |
| H | -3.816000 | -1.094000 | 1.208000 | H | 3.816000 | 1.103000 | 1.202000 |
| P | -2.383000 | 1.205000 | -1.195000 | H | 2.361000 | 2.644000 | 1.107000 |
| H | -2.359000 | 2.638000 | -1.125000 | H | 2.239000 | 1.156000 | 2.616000 |
| H | -2.243000 | 1.138000 | -2.622000 | H | 0.000000 | -1.087000 | 0.002000 |
| H | -3.816000 | 1.099000 | -1.203000 | H | -0.000000 | 1.087000 | -0.003000 |